12-1994

An Investigation and Improvement of Electrorheological (ER) Fluid Technology

Adil F. Dalal

AN INVESTIGATION AND IMPROVEMENT OF ELECTORHEOLOGICAL (ER) FLUID TECHNOLOGY

by

Adil F. Dalal

A Thesis
Submitted to the
Faculty of The Graduate College
in partial fulfillment of the
requirements for the
Degree of Master of Science in Engineering
Department of Mechanical and Aeronautical Engineering

Western Michigan University
Kalamazoo, Michigan
December 1994

ACKNOWLEDGEMENTS

There are no words which can express my gratitude towards those involved in the completion of my thesis. The most important contribution was that of Dr. Haenicke, the president of WMU, whose generous grant for instrumentation was a major factor in keeping this research alive. I sincerely thank you Dr. Haenicke.

I also wish to thank all my committee members Dr. R. Hathaway, Dr. P. Merati, Dr. D. VandenBrink (MAE), Dr. M. McCarville (Chemistry) and Dr J. Gesink (EE) for their advice and support during the course of this thesis. My special thanks to my advisor, Dr. R. Hathaway, an extremely experienced and reputed researcher, under whose mentoring, I was allowed to make independent decisions and was successful in guiding my research to a suitable conclusion.

I thank the technicians, Pete Thannhauser, Mark Ely (MAE) and Glen Hall (ET), who provided adequate support for the construction of my apparatus and in instrumentation. I also thank the supplier of ER fluids, a company which considers information relating to the fluids as proprietary, and requests confidentiality of all the information supplied. Above all, I thank my parents whose moral support was invaluable in the success of this research.

Adil F. Dalal

AN INVESTIGATION AND IMPROVEMENT OF ELECTORHEOLOGICAL (ER) FLUID TECHNOLOGY

Adil F. Dalal, M.S.E.

Western Michigan University, 1994

The purpose of this research was to investigate and overcome the limitations of Electrorheological (ER) fluids and to introduce this advanced technology at WMU. Electrorheological (ER) Fluids are a special class of fluids, which exhibit a reversible, infinitely variable phase transition from a liquid to a solid/semi-plastic state, in the presence of an electric field.

ER fluids can provide a unique solution to the problems of vibration isolation of systems. The applications are currently limited due to the high voltage requirements, electric power related heating and limited research into wear/abrasive characteristics of ER fluids.

A specially designed and constructed "electro-viscosimeter" and power source, were employed to determine the optimal electric signal, reduce the power input and the resulting fluid temperatures of ER fluid components. The research should prove invaluable in the advancement of the current applications of ER fluids. It should also lead to introduction of innovative applications of ER fluids.

TABLE OF CONTENTS

CHAPTER

CHAPTER

CHAPTER

LIST OF TABLES

LIST OF FIGURES

List of Figures-Continued

CHAPTER I

PROJECT SUMMARY

Objective of the Proposed Research

The first objective of the research was to study the physical behavior of electrorheological (ER) fluids. Electrorheological fluids are fluids whose physical properties can be altered in the presence of an electrical field. This characteristic enables these fluids to become part of active or smart systems and mechanisms. The research focused on those properties of the ER fluids that allow or inhibit their use in mechanical systems.

An additional objective of the research was to investigate the effect of the excitation waveform on the fundamental characteristics of shear stress, shear rate by employing frequency and pulse-width modulation and to investigate the effect of temperature on the shear stress-electric field relationship.

A "viscosimeter", specially designed and constructed by me as a part of the thesis, was employed to evaluate the characteristics of the electrorheological fluids. The work plan for the research was as shown in Table 1.

Summary of Results

The experiments were carried out at voltages of 1, 1.5 and 2 kV, frequencies

ranging from 100 to 11000 Hz, pulse-widths ranging from 0.02 to 7.5 milliseconds and duty- cycles of 25%, 50% and 75% for a particular ER fluid which was responsive to an A.C. electric field only. The results obtained may or may not be true for test conditions other than those considered and for other ER fluids. The shear stress was observed to increase with increasing field strength and showed a drop with increasing frequency. The efficiency factor was observed to drop with increasing frequency and voltage. Equations were developed for shear stress and efficiency factor as a function of frequency, duty cycle, voltage and pulse-width. The major factors affecting shear stress and efficiency factor were voltage and pulse-width. Under the experimental conditions, maximum shear stress and maximum efficiency factor were observed at voltages of 2 kV and 1 kV respectively, both occurring at pulse-width of 7.5 ms and frequency of 100 Hz (i.e. at 75% duty cycle).

Table 1

Work Plan

SUMMER 1993	To finalize the construction of the "electro-viscosimeter" and to undertake the instrumentation and calibration.
FALL 1993	Procurement of the ER fluid and power source. Preliminary testing of the fundamental properties of ER fluids.
WINTER 1994	Determination of optimum electrical waveform and evaluation of voltage-frequency dependence.

CHAPTER II

PROJECT DESCRIPTION

Introduction

In 1939, W. M. Winslow discovered a remarkable phenomenon, that, when a special class of fluids are subjected to a strong electric field, they tend to solidify instantly. This change was observed to be completely reversible i.e. the solid would revert back to liquid behavior as soon as the electric field was removed (Winslow, 1949).

These special class of fluids, which exhibit a reversible change in rheological properties, in the presence of an electric field, are known as electrorheological (ER) fluids. This infinitely variable 'phase transition' from a liquid state to a solid/semi-plastic state occurs in less than ten milli-seconds.

The favorable response times of the fluids provide versatility in application and control of mechanisms. This characteristic enables the fluid to become a part of active or smart systems and mechanisms. ER fluids allow direct control of devices via electrodes inserted into the fluid. This results in the elimination of force transmission through complicated interfaces like mechanical linkages and/or clutches. The prime advantages of ER fluids are; fast response, significant reduction in space and weight, simpler devices with improved reliability and a low power consumption.

Potential applications of ER fluids are almost without limit. The automotive industry is envisaged to be the prime benefactor of ER fluid technology. Active suspension systems, automatic transmissions, clutches and braking systems, actuators, hydraulic valves and vibration dampers are all applications being studied and developed. ER fluids also have a great scope of application in defense (Gandhi & Thompson, *Smart Materials & Structures*) and in prosthetic apparatus (Stangroom J.E., "Electrically Variable Linkage Joints").

Electrorheological Response

The transformation from fluid to solid and the subsequent increase in suspension stress transfer by many orders of magnitude upon the application of an electric field is known as an ER effect or response.

Description

The mechanics of ER effect are not completely understood, however, it is believed that the solid particles form fibrous structures which align like chains in the direction of the applied field. Thus, the ER effect is believed to be partly dependent on the polarization of the solid particles (Gast & Zukoski, 1989a).

ER fluids are composed of a suspension of highly polarizable, microscopic, porous particles of hydrophilic solids in non-polar, hydrophobic liquids. The solid particles, which may be organic or non-organic having a diameter ranging from 1 μ to 50 μ, are the "active" particles which are responsible for the ER effect. The

known liquid component is usually a mixture of hydrophobic vehicles, including oils and halogenated hydrocarbons, having a low conductivity (Gast & Zukoski, 1989b).

In the absence of an electric field, the ER fluids behave in a Newtonian manner with the shear stress (force applied per unit area) directly proportional to the shear rate (relative velocity per unit thickness). With no electric field present, a small force will make the fluid flow. In the presence of an electric field, no flow occurs and the solid state of the electrorheological fluid is characterized as a Bingham plastic. In this state, if the mechanical stress is increased, a yield point is reached where the gel breaks down and flow commences at an increased viscosity. Figure 1 (Gast & Zukoski, 1989b) shows a plot of shear stress versus shear rate for an ER fluid, where EF is the applied electric field.

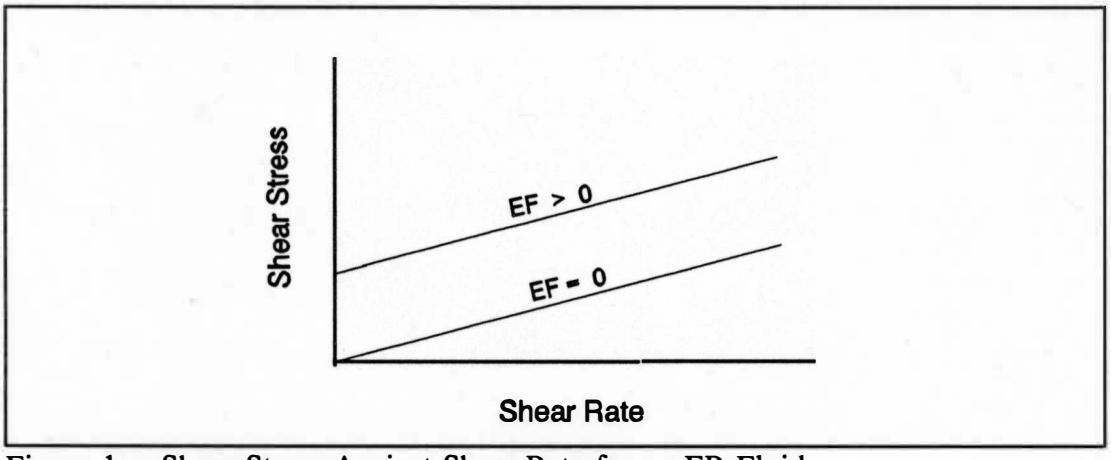

Figure 1. Shear Stress Against Shear Rate for an ER Fluid.

CHAPTER III

POTENTIAL APPLICATIONS AND LIMITATIONS OF ER FLUID TECHNOLOGY

Potential Applications

The potential applications of ER fluids are unlimited, ranging from automobiles to prosthetic devices. ER fluids would provide a major breakthrough in the vibration isolation problems in automobiles. Researchers believe that engine and transmission mounts using ER fluids would provide an active dampening of excessive vibration and active control of noise, vibration and harshness. ER fluid dampers would be made to respond not only to velocity of the load but also to displacement and acceleration, thus providing a "fully active" suspension system. The automotive industry is envisaged to be the prime benefactor of ER fluid technology. Active suspension systems, automatic transmissions, clutches, braking systems, actuators, hydraulic valves and vibration dampers are all applications being studied and developed.

ER fluid technology also finds importance in electrically variable linkage joints as applicable to robots and artificial human limbs for physically handicapped (Stangroom). ER fluids would provide a multi-directional, millisecond response to an applied electric field in the electrically variable linkage joints (Dalal, 1989).

ER fluid research is a priority with the U.S. Defense for the development of "active sensing and smart structural systems". Actuators like ER fluids, optic fibers and piezoelectric materials along with a network of sensors and microprocessors would provide autonomous and controlled changes in the shape, mass, stiffness, energy-dissipation and dynamic response characteristics of the "smart" structures. However, the preference is for the nonmechanical materials like ER fluids due to their ability to physically deform themselves (Brown, 1990).

The ultimate application of ER fluids is envisaged in building adaptive intelligence in materials through a network of sensors, which allow monitoring aircraft health and flight worthiness. Gandhi and Thompson believe that ER fluids, along with a sensor network, would provide "smart" wings which would change the natural frequency of the wing structure relative to the consumption of aviation fuel and monitor ice build up on the wings and control surfaces. ER fluids would also find applications in an active damping system for missile flight-control actuation systems. Researchers are currently working on the design of automatic transmissions, of the Continuously Variable type (C.V.T.), using ER fluids (1988). The U.S. Army is considering running channels of ER fluids through helicopter rotors to control the stiffness of each blade independently, in order to reduce vibration and compensate for damage (Brown, 1990). Composite materials, embedded with ER fluids (Gandhi et al, 1989), are being used to dampen monitoring devices, SDI weapons, telescopes and other space structures requiring extreme accuracy.

Current Limitations

The potential applications of ER fluids are almost unlimited. However, the high voltages required to solidify ER fluids, the power consumption and the subsequent degradation of the fluids, is the major impediment in the implementation of ER fluid technology to a broad spectrum of devices. An in-depth study to determine the optimum electrical waveform and voltage combination is thus important to determine the optimum voltage and frequency ranges for efficient functioning of the ER fluids. The increase in temperatures at high voltages is detrimental to the overall performance of the ER fluids and to the device which employs the fluids. The life and maintenance requirements of ER fluid devices are limited by the abrasive characteristics of ER fluids. A thorough investigation of the dependence of ER response on voltage and temperature and a detailed study of the abrasion tendencies, which are a function of the fluid suspensions, will provide valuable information needed for potential new applications.

The following characteristics of ER fluids need to be carefully studied, in order to apply the ER fluid technology to mass production devices: (a) Power requirements, (b) Temperature effects and (c) Lubricating characteristics.

Power Requirements

Electric fields have a strong effect on the ER fluid performance. Researchers have investigated the dependence of ER fluid performance on the frequency of the

applied electric fields (Klass & Martinek, 1967 a & b). The application of an AC electric field to the ER fluids resulted in the degradation of the fluids and increased power consumption. These effects were reduced by the use of a pulsed DC (Stevens, Spatrston & Stanway 1985).

At present ER fluids require a high voltage of approximately 5-10 kV/mm gap at a current of 5 mA. However, in order to be able to make ER fluid technology safe and cost-effective and to make efficient use of ER fluid systems in automobiles and prosthetic devices, the power consumption of ER fluids need to be further reduced. The effect of frequency modulation and pulse-width modulation, which may be an answer to the above drawback, had not yet been studied prior to this research.

Temperature Effects

The effect of temperature on ER response needs careful investigation. Brief tests, which have been carried out so far, indicate an increased ER response with increasing temperatures (Klass & Martinek, 1967 a & b). However, since the results were based on readings taken only at two temperatures, more tests are required to support the above results.

Lubrication Characteristics

The life and maintenance of ER fluid devices depends on lubrication/abrasive characteristics (Lingard et al, 1989) of ER fluids. This research is to be undertaken by Dr. Stangroom and others (Stangroom, Fax, Dec 12,1992) in Germany.

CHAPTER IV

TEST APPARATUS, INSTRUMENTATION AND CALIBRATION

Test Apparatus

The apparatus used is shown schematically in Figure 2. It was specially designed and constructed as a part of the master's thesis. This "viscosimeter" would be used to test the ER response of the fluid under varying parameters of voltage, frequency and signal shape.

The experimental set-up consisted of :

1. Variable Speed Motor Drive: A 3/4 HP, 1720 rpm AC motor was used to power the spindle. Through fixed and variable drive systems a spindle speed range of 100-850 rpm was achieved.

2. Electrodes:

   (a) Upper Electrode. The upper electrode (Figure 3) consisted of a disk held in the drill chuck. It was immersed in the ER Fluid to a pre-determined depth. The depth of immersion determined the gap between the lower and upper electrodes.

   (b) Lower Electrode. The lower electrode (Figure 4) consisted of a stationary electrode immersed in an insulated beaker.

3. Strain Measurement Fixture: A specially designed fixture consisted of a

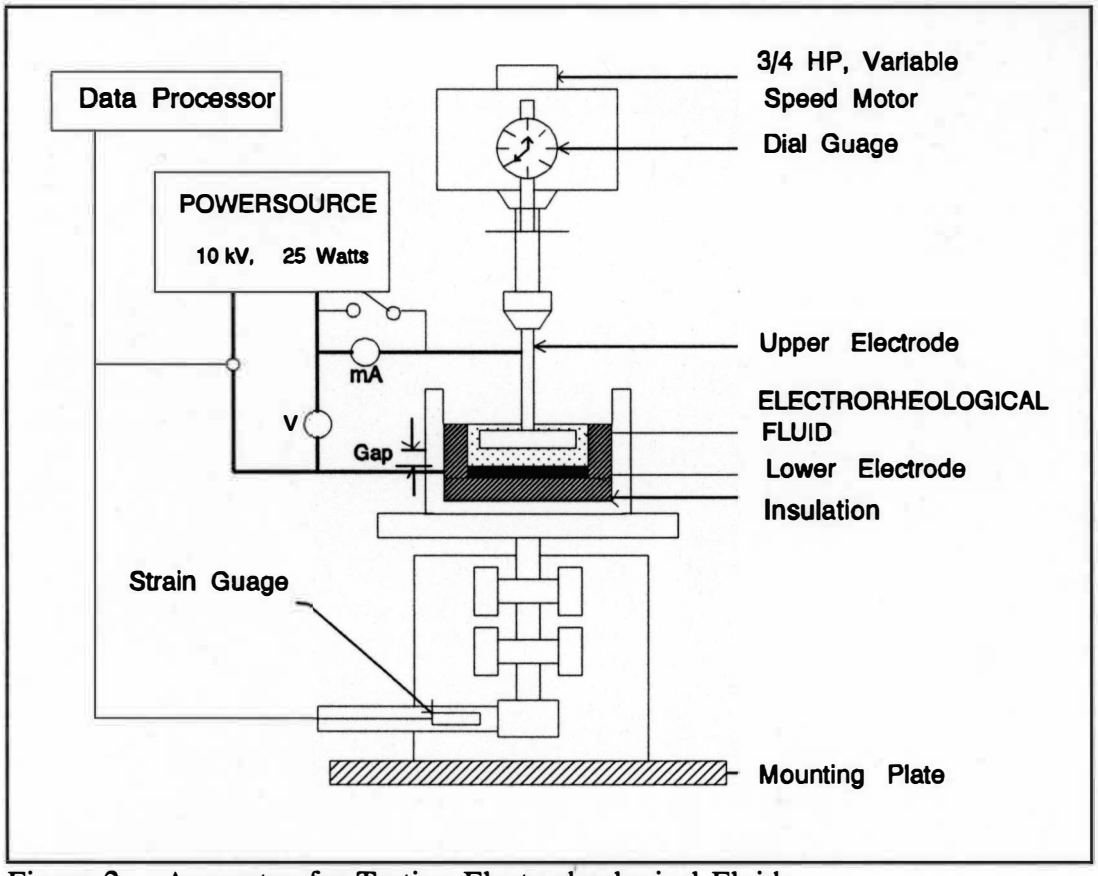

Figure 2. Apparatus for Testing Electrorheological Fluids.

plate on which the beaker was placed. The plate was rigidly attached to a shaft which was held in 2 self- aligning, anti-friction bearings. At the other end of the shaft was attached a strain gauge in order to measure its deflection and thus the torque transmitted by the ER fluid. The entire assembly was held rigidly in the X, Y, Z planes while allowing angular deflection as a function of load against the strain beam.

4. A Dial Gauge: A dial gauge, calibrated to read displacement with an accuracy of one thousandth of an inch, was attached to the vertical adjustment table of the machine and was employed to control the gap between two electrodes.

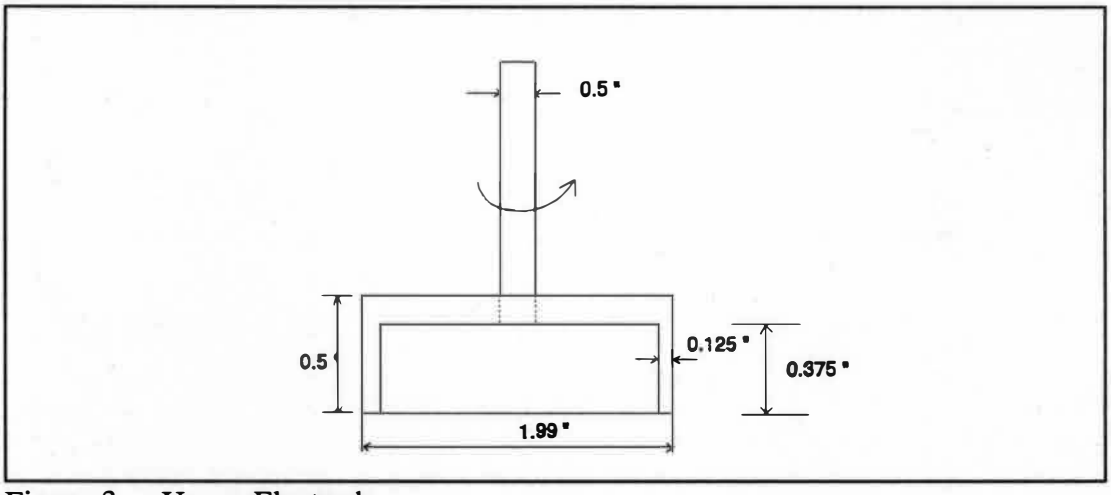

Figure 3. Upper Electrode.

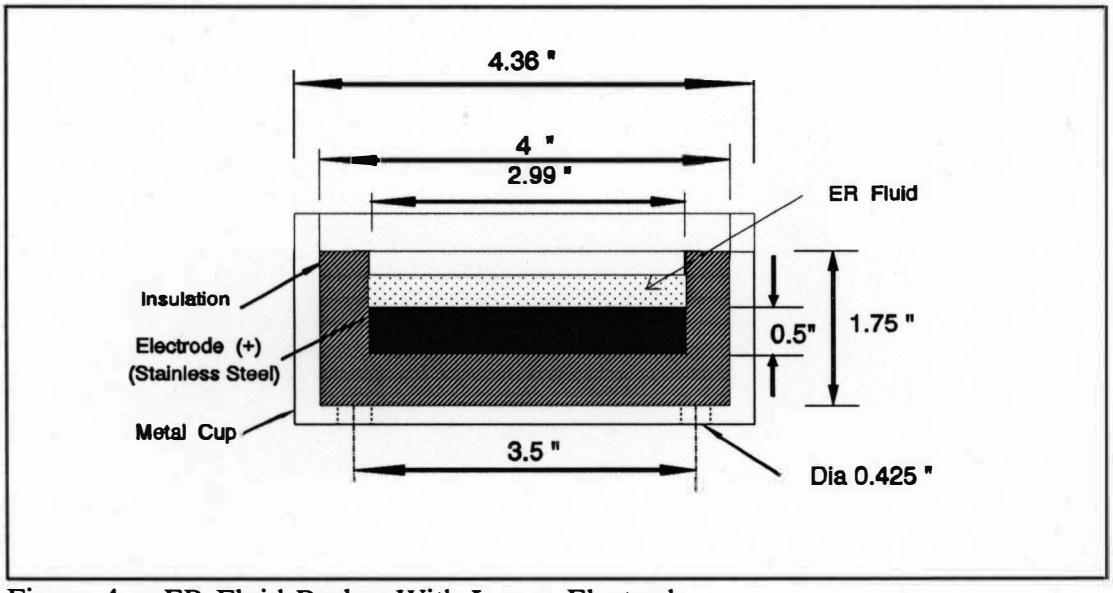

Figure 4. ER Fluid Beaker With Lower Electrode.

5. Induction Pick-Up: An induction pick-up in conjunction with a 60 tooth gear, was used to indicate the output speed of the spindle. The shear rate could thus be determined as a function of the angular velocity of the spindle.

6. Thermocouple and Thermocouple To Millivolt Converter: A thermocouple inserted into the beaker containing the ER fluid, provided a continuous read-out of

the temperature. A thermocouple to millivolt converter provided a linearized signal to the analog to digital interface and card.

7. Computer with an Analog-Digital board and Software: A computer with an Analog-Digital board and specially developed software was used to collect and plot the experimental data for the various fluids.

Instrumentation, Calibration and Calculations

Measurement of Shear Rate

The shear rate measurement was conducted by bolting a 60 tooth gear onto one of the pulleys of a pulley-system attached to a variable speed motor. An Induction-pickup, with the help of a bracket, was placed very close to the toothed gear. The induction pickup magnetically picked up a signal from each tooth and sent it to the "Frequency In" socket of the "Frequency to Voltage circuit box" (Figure 5), which was powered by a 9V 500 mA DC supply. The output voltage was fed from the "Voltage Out" socket to the Analog to Digital interface. Using analysis software, the rpm was read and was calibrated to provide the strain rate in units of 1/second.

The frequency to voltage circuit employed, was a monolithic frequency to voltage converter with high gain op amp/ comparator designed to operate a load when input frequency reached or exceeded a selected rate. The tachometer used a charge pump technique and its output swung to ground for a zero frequency input. The "Frequency to Voltage Circuit" is shown in Figure 7. The output voltage was given

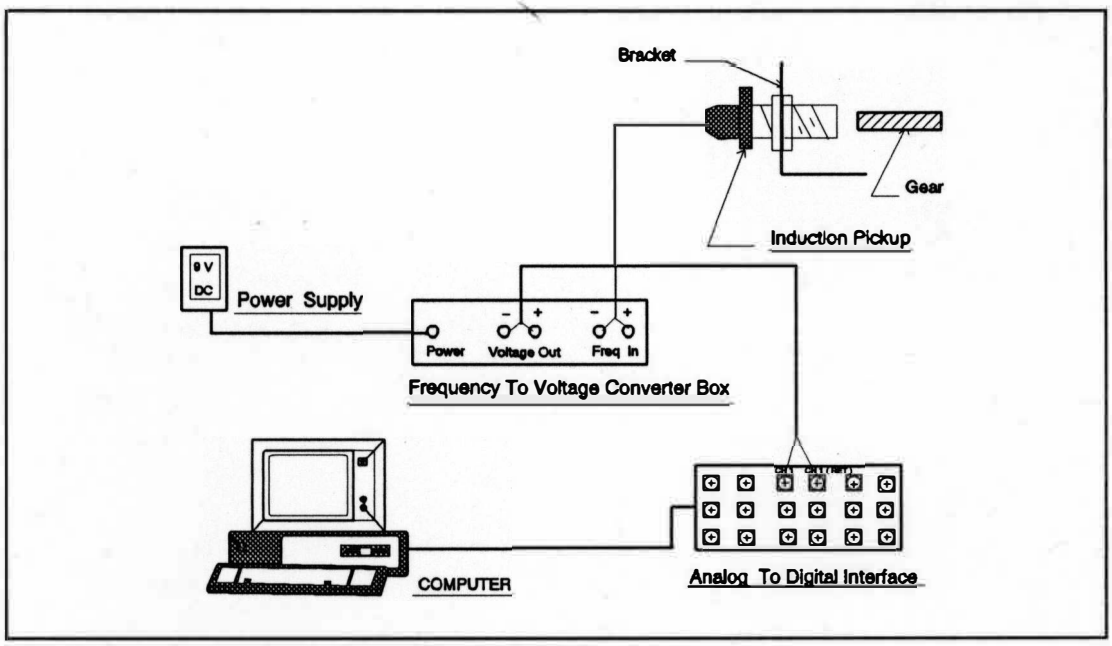

Figure 5. Set-up for Measurement of Strain Rate.

by Equation 1, where,

$$V_{OUT} = f_{INP} \times V_{cc} \times R1 \times C1 \qquad (1)$$

V_{OUT} = Output voltage

f_{INP} = Input frequency from the induction pickup

V_{cc} = Input voltage

R1 = Resistance value and C1 = Capacitance value

The values of R1, C1 and C2 could be varied for different frequency ranges. For a frequency range of 100-1500 cps, the resistance and capacitance values selected were R1 = 50 K, C1 = 0.01 μF and C2 = 1 μF. It was very important that an input not go below ground without some resistance in its lead to limit the current that

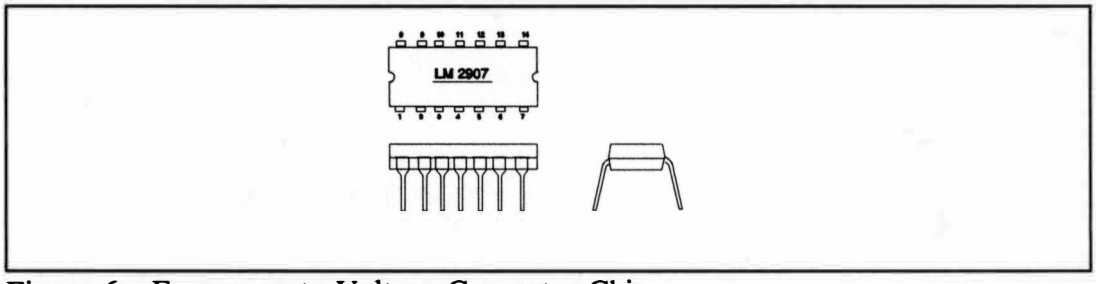

Figure 6. Frequency to Voltage Converter Chip.

would flow in the episubtate diode.

Shear Rate Calibration and Calculation

The shear rate was calibrated by the use of 2 induction pick-ups. One of the induction pickups took the signal from the 60 tooth gear, through channel 1 of an analog to digital interface to an analog to digital card in the computer. Using the software developed, the output of a data value was obtained. The data value obtained was calibrated to read rpm by the use of a second induction pickup, which read rpm directly by the use of a tachometer. A regression analysis was carried out on the data value (X-axis) and the actual speed (Y-axis) values. The calibrated rpm was obtained by substituting the "Constant" and "X Coefficient", obtained from the regression analysis, in the equation of a straight line. The measured rpm and the calibrated rpm were very close as observed from the graph shown in Figure 8. The shear rate was obtained by using Equations 2 and 3, where,

w = Angular velocity (rad/sec)

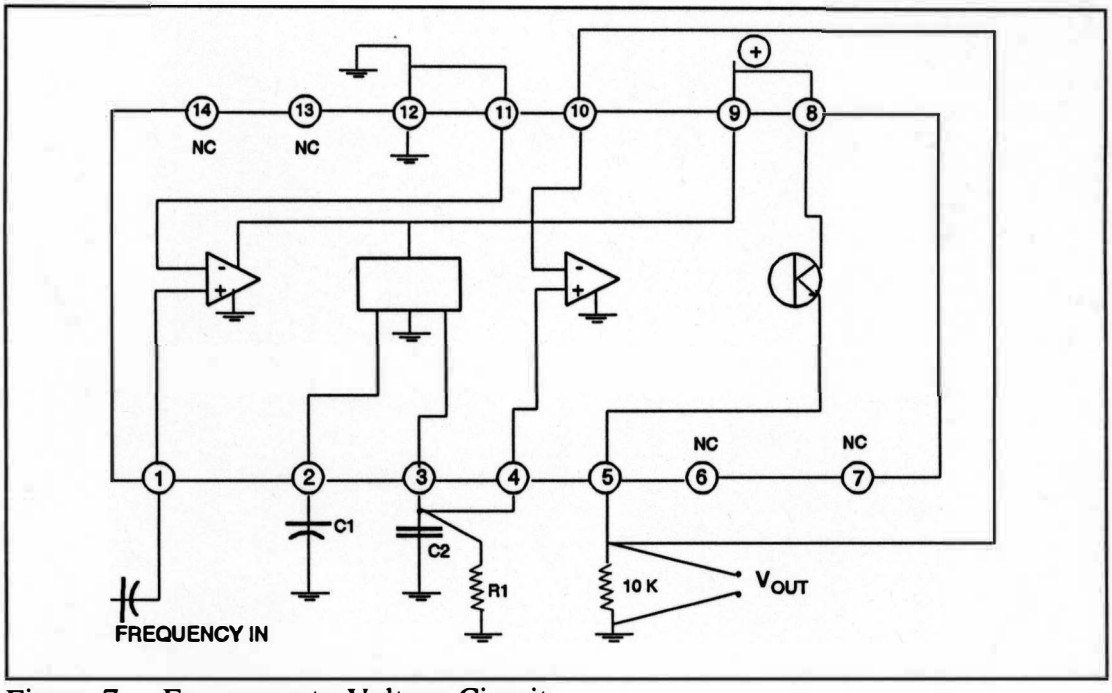

Figure 7. Frequency to Voltage Circuit.

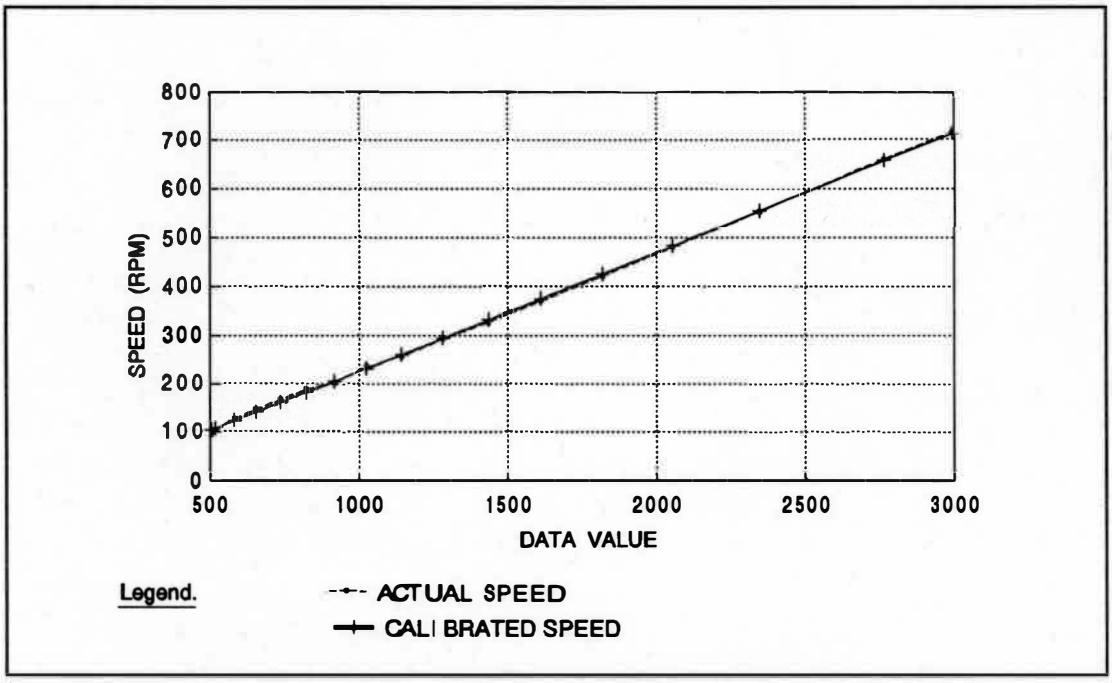

Figure 8. Comparison of Actual Speed and Calibrated Speed.

$$\gamma = \frac{w\, r_m}{h} \quad (rad/\text{sec}) \tag{2}$$

$$\gamma = \frac{N_c\, r_m}{60\, h} \quad (1/\text{sec}) \tag{3}$$

r_m = Mean radius of upper electrode (m)

h = Gap between the upper & lower electrodes

N_c = Calibrated speed (rpm)

Measurement of Shear Stress

The shear stress of the fluid was measured by means of a beam having four strain gauges (i.e. two in tension and two in compression). As shown in Figure 9, the beaker containing the ER fluid was welded to a shaft which was supported in two anti-friction bearings which were rigidly attached to a plate. The entire assembly was held to allow rotation only, and the deflection of the beam provided a measure of the torque exerted on the fluid and could thus be calibrated to read shear stress directly.

The resistive strain gauges were connected to the strain indicator at the binding post on the front panel. Figure 10 shows input connections for full-bridge configuration. The output from the strain indicator was taken into analog to digital interface.

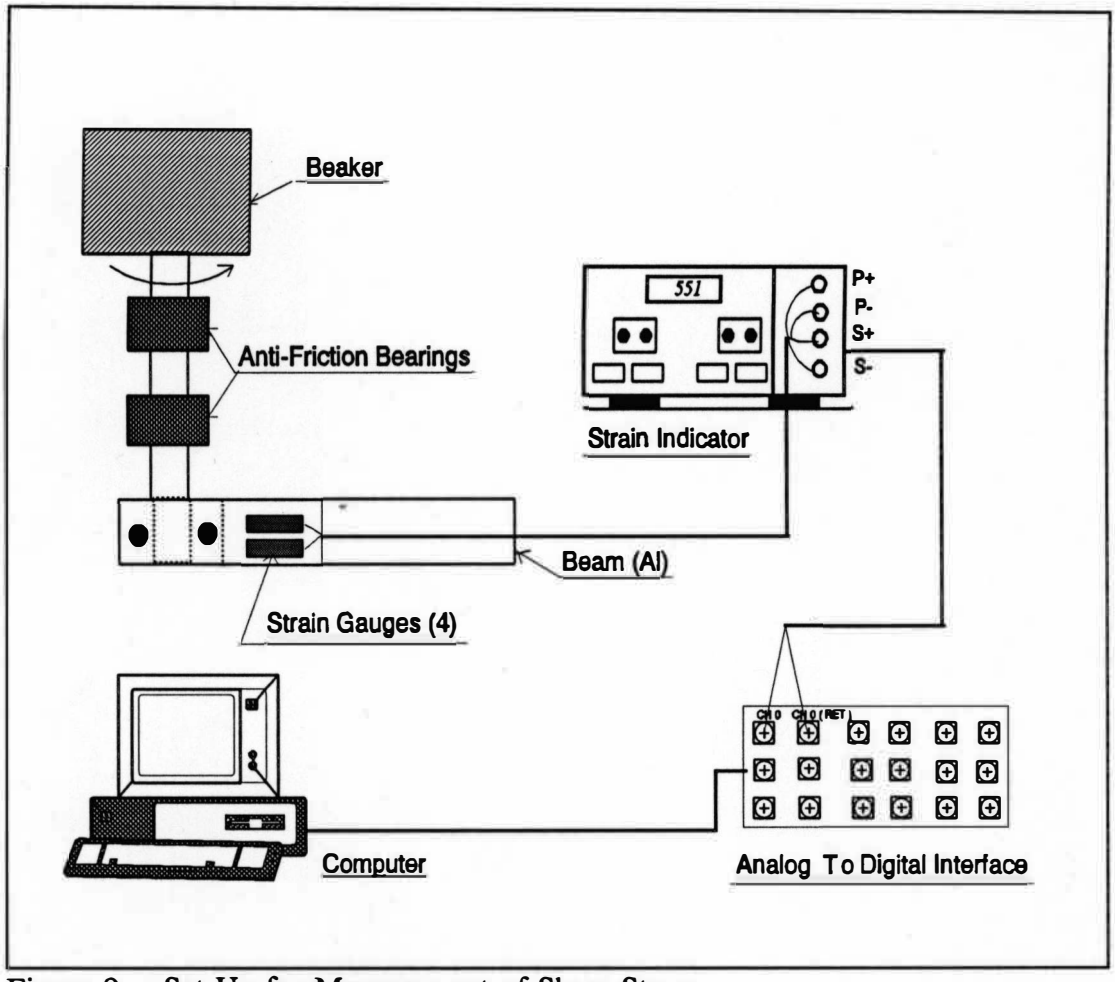

Figure 9. Set-Up for Measurement of Shear Stress.

Shear Stress Calibration and Calculation

The shear stress was calibrated by the use of a chord and a pulley system. A string wrapped tightly around the beaker containing the ER fluid and the other end of the chord was passed through a pulley and weights were suspended from it. For different weights, the torque exerted changed and thus the deflection of the stain beam also varied, and the value of the torque obtained from the computer with the

analog to digital interface. The data value obtained could be calibrated to read the actual torque by comparing it with the theoretical torque. The calibration set-up is shown in Figure 11. A regression analysis was carried out on the data value (X-axis)

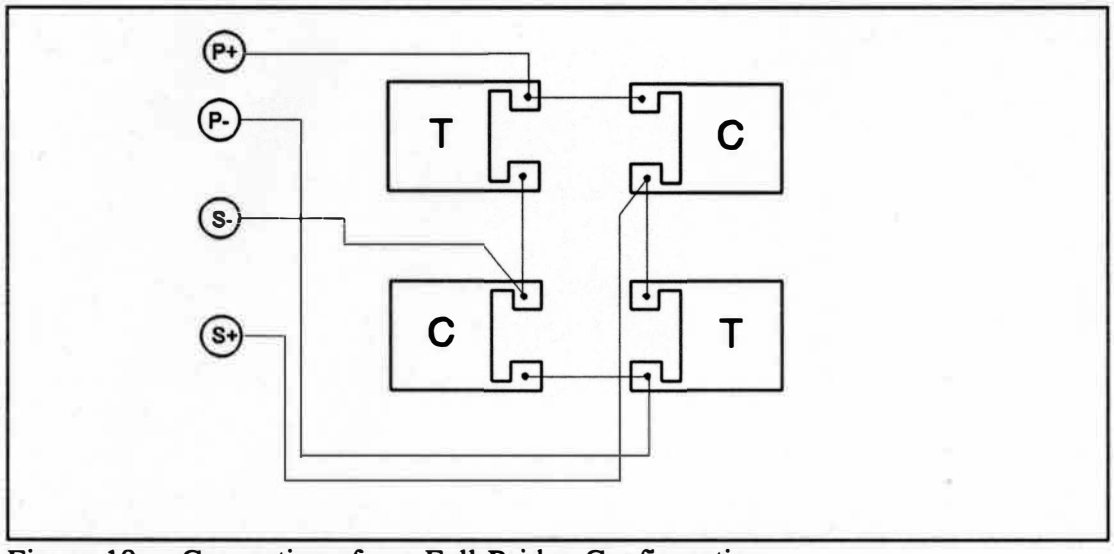

Figure 10. Connections for a Full-Bridge Configuration.

and the actual torque (Y-axis) values. The calibrated torque was obtained by substituting the "Constant" and "X Coefficient", obtained from the regression analysis, in the equation of a straight line. The shear stress was calculated by using Equation 4. The graph comparing the values of the actual shear stress and the calibrated shear stress is shown in Figure 12. The shear stress was obtained by using the Equation 4.

$$S_s = \frac{T}{A_d\, r_m}(Pa) \qquad (4)$$

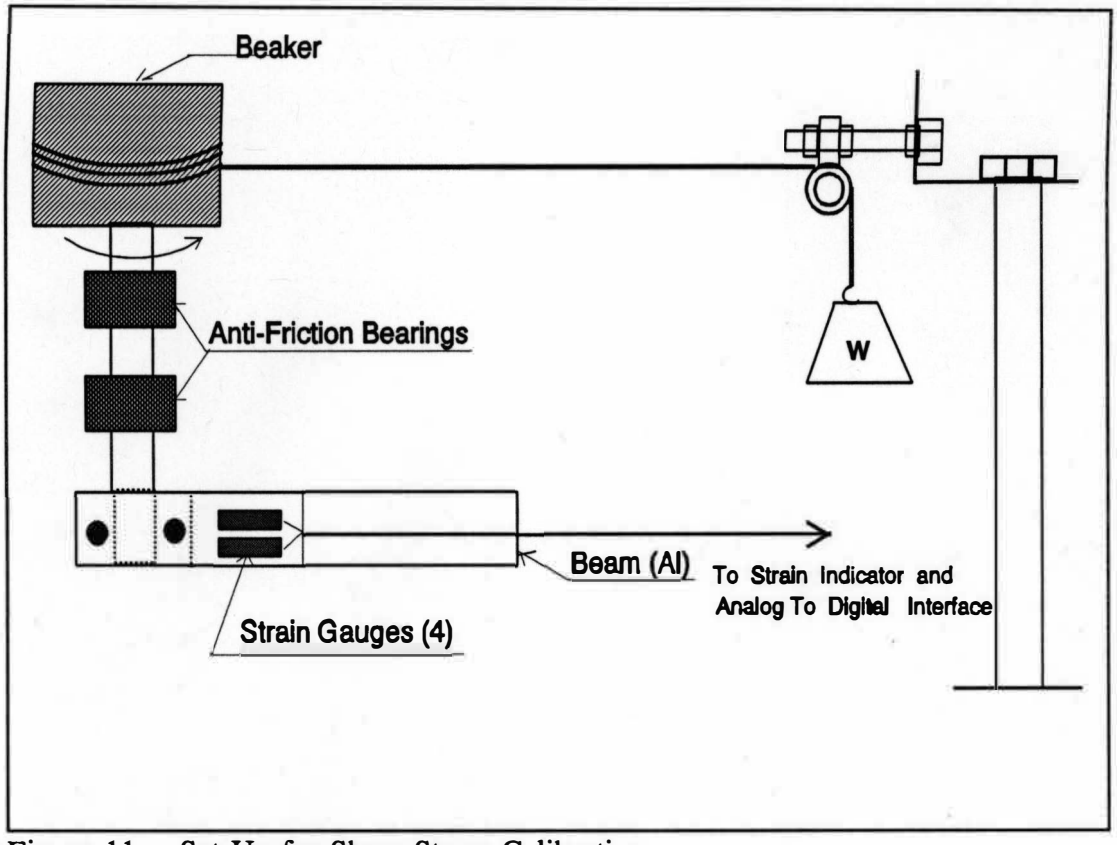

Figure 11. Set-Up for Shear Stress Calibration.

T = Torque exerted on the fluid (N.m)

A_d = Area of the upper electrode (m^2)

r_m = Mean radius of upper electrode (m)

Measurement of Temperature

The temperature of the ER fluid was measured during the course of the experiments. One end of a thermocouple wire was kept in contact with the ER fluid in the beaker. The other end of the thermocouple was connected to a thermocouple to millivolt converter which was calibrated to read 1 millivolt/degree. The

temperature values from the converter to the analog to digital interface in the computer. The experimental set-up for temperature measurement is shown in Figure 13.

The TAC30 (OMEGA Engineering Inc.) was a portable thermocouple to analog converter which converts a chart recorder or analog to digital voltmeter into an accurate and wide range temperature measuring instrument. It amplified and linearized the signal and provided a precision 1 mV/°C or °F signal for a thermocouple. It also provided a cold-junction compensation.

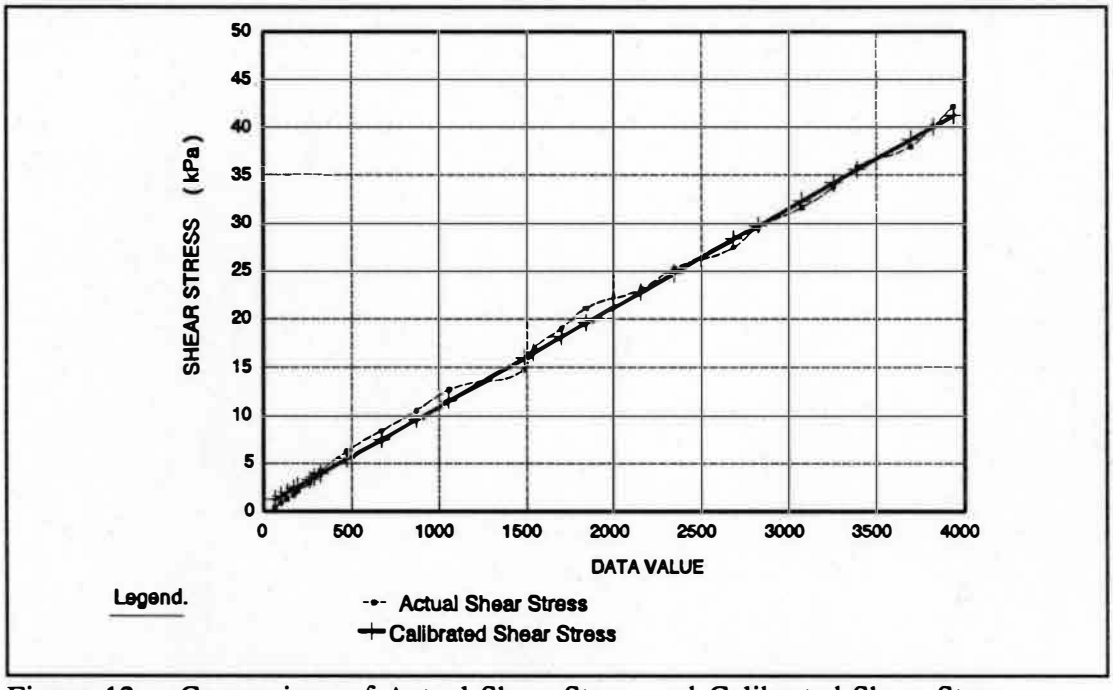

Figure 12. Comparison of Actual Shear Stress and Calibrated Shear Stress.

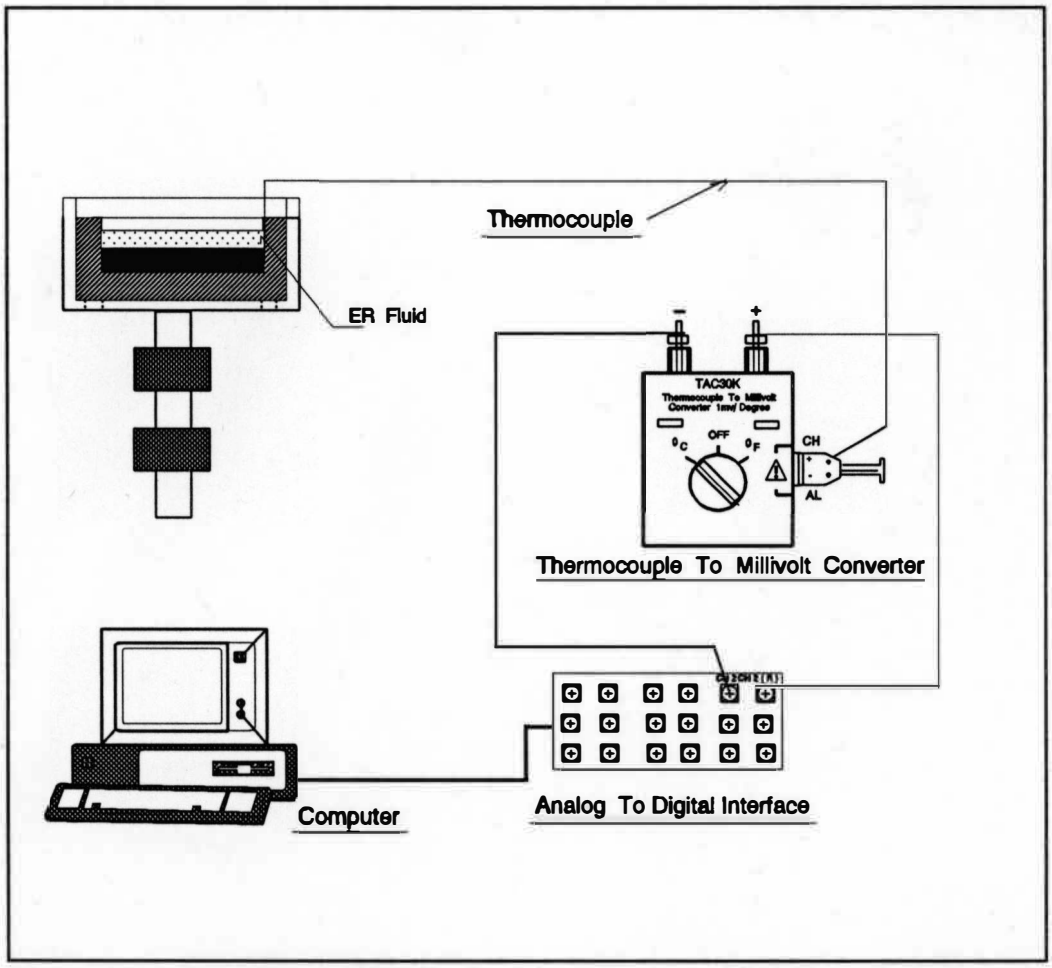

Figure 13. Experimental Set-Up for Measurement of ER Fluid Temperature.

Temperature Calibration and Calculation

A thermometer and the free end of the thermocouple was simultaneously dipped into the water and the data value read of the computer was compared to thermometer reading. The calibration set-up is shown in Figure 14. A regression analysis was carried out on the data value (X-axis) and the actual temperature (Y-axis) values. The calibrated temperature was obtained by substituting the "Constant"

and "X Coefficient" in the equation of a straight line. The plot of the actual temperature and the calibrated temperature is shown in Figure 15.

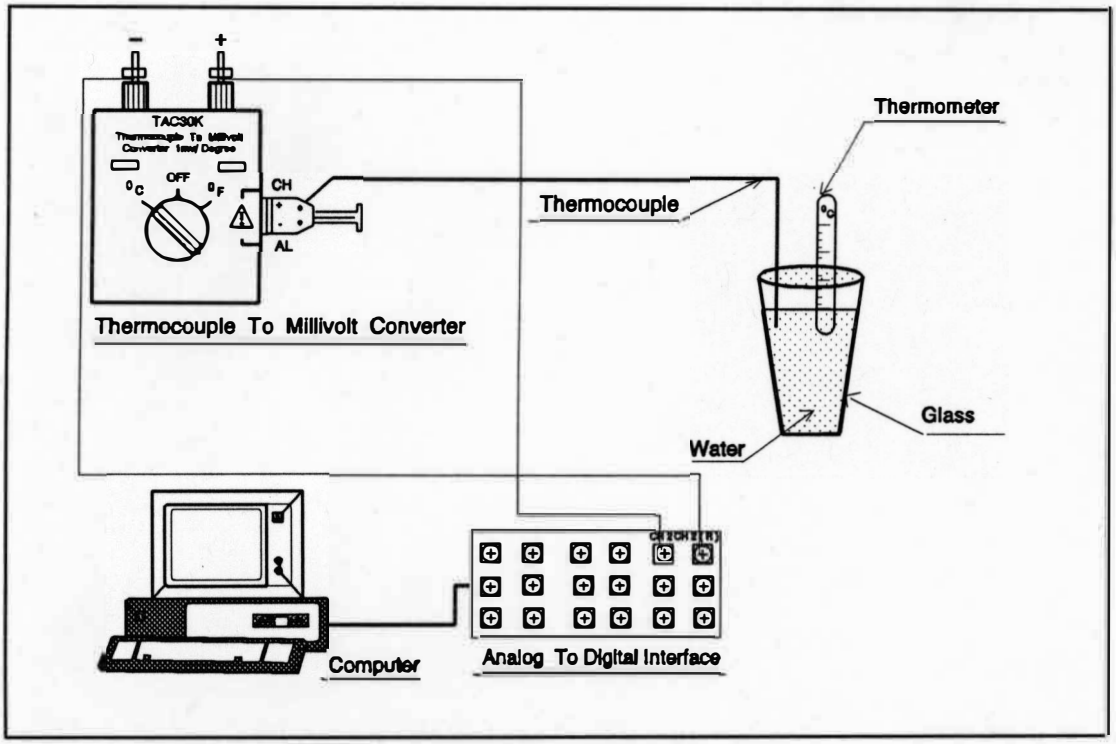

Figure 14. Set-Up for Calibration of Temperature.

The Temperature in °F was obtained by using the Equation 5, where,

Tc = Temperature (oC)

$$T_F = 1.8\ Tc + 32 \qquad (5)$$

10 kV Power Source and 10 k-C Pulser

The power source used was an EH series, 100 watt regulated high voltage dc

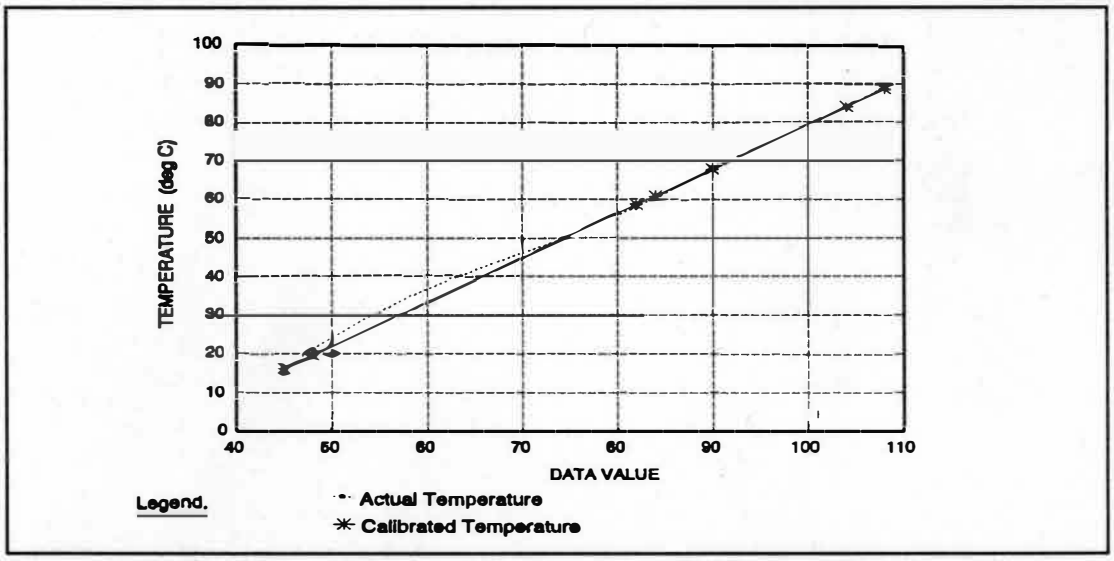

Figure 15. Comparison of Actual Temperature and Calibrated Temperature.

power supply made by Glassman High Voltage Inc.

The model 10k-C is a 10 kV pulse generator which is primarily designed to capacitive loads. The specifications provided for this equipment were quite complex which included a variable frequency, pulse width, duty cycle, voltage and current ranges. This pulser was not commercially available and was specifically designed by Instrument Research Company (IRCO) for the purpose of this thesis. It basically consists of two hard tube switches: one to charge the capacitive load and the other to discharge the capacitance providing a fast fall time. It has a variable pulse amplitudes from 0 to 10,000 volts and variable pulse widths from 1 microsecond to dc.

CHAPTER V

METHODOLOGY OF EXPERIMENTATION

Aim of the Experiment

The aim of the experiment was :

1. To investigate the dependence of wave-form and frequency of an applied electric field on the mechanical properties of ER fluids response of ER suspensions on the electric field, by employing pulse-width and frequency modulation.

Dependence of Electric Wave-Form

ER Fluid, contained in the gap defined by the upper and lower electrode, was subjected to a voltage varying from 0 to 10 kV/mm. The thickening of the fluid in the presence of an electric field causes the supporting shaft to rotate against the strain measuring beam. The beam deflects due to the torque and the strain gauge will strain as a function of torque which will be used to calculate the shear stress developed in the fluid. The stress beyond a critical shear rate is described by Equation 6.

$$T = T_B + \eta_{pl}\, r \qquad (6)$$

The slope of the line described by Equation (6) gives the plastic viscosity η_{pl} and the intercept of the line is equal to the Bingham yield stress T_B. The shear rate (r) is a

function of the angular velocity of the upper electrode. The effect of electrical signal shape on efficiency is given by Equation 7. In the experiments conducted Response was the shear stress (kPa) obtained due to the applied electric field and the power input was the electric power consumption of the ER fluid (milliwatts).

$$Efficiency = \frac{Response}{Power\ Input} \tag{7}$$

The ER Effect was tested using varying voltage, current, frequency, pulse width and thus the duty cycle of the wave-forms. An example of the square wave form to be used is shown in Figure 16.

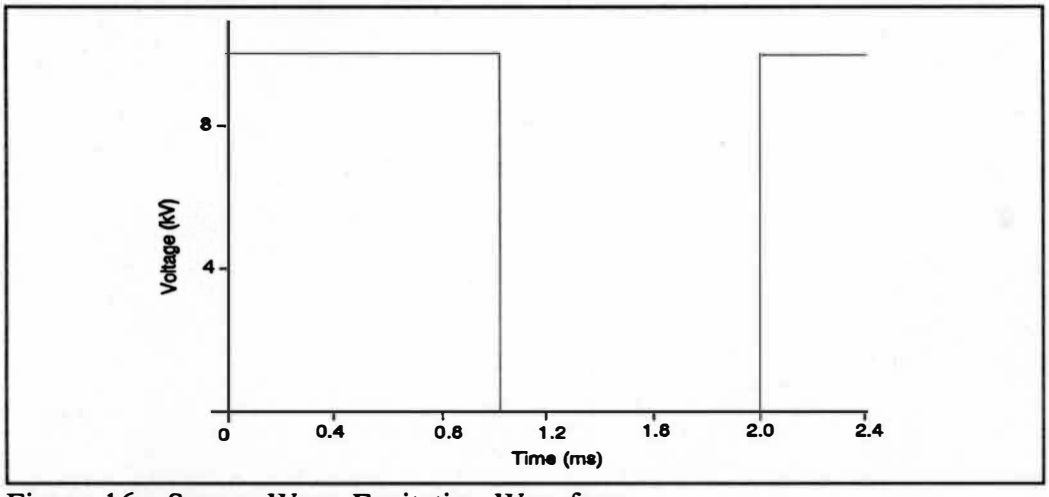

Figure 16. Square-Wave Excitation Waveform.

The general procedure used was that, out of the following parameters, some of them were kept constant and the others were varied as required: (a) Speed (rpm) of rotation of the upper electrode, (b) Voltage (kV), (c) Frequency (Hz) of the wave-form and (d) Pulse width (milliseconds) of the wave-form.

The data collected included the following parameters: (a) Shear stress (kPa), (b) Shear rate (1/second), (c) Temperature (degree F) and (d) Electric Power Consumption (milliWatts).

CHAPTER VI

EXPERIMENTAL DATA AND RESULTS

Test 1

Objective (Test 1A)

The objective of this test was to determine the dependence of shear stress on frequency at different voltages. The gap and speed were held at a constant value. The readings of shear stress were taken at variable frequency, voltage and duty cycle settings.

Test Conditions

Table 2

Test Conditions (Test 1)

VOLTAGE	1, 1.5 and 2 kV
DUTY CYCLE	25%, 50% and 75%
FREQUENCY	100 to 11000 Hz
GAP	0.04 in
SHEAR RATE	233 1/s
$TEMP_{start}$	72 ^0F
$TEMP_{end}$	76 ^0F

Experimental Data

The shear stress data for duty cycles of 25%, 50% and 75% is shown in Tables 3, 4 and 5 respectively.

Table 3

Shear Stress Data (25% Duty Cycle)

		SHEAR STRESS		
Frequency	Pulse Width	1 kV	1.5 kV	2 kV
(Hz)	(ms)	(kPa)	(kPa)	(kPa)
100	2.5	0.7903	0.9254	1.0306
200	1.25	0.8311	0.8934	0.9269
500	0.5	0.8293	0.9146	0.976
1000	0.25	0.7983	0.8679	0.9447
2000	0.125	0.8037	0.840911	0.9563
3000	0.083333	0.8222	0.8193	0.9212
4000	0.0625	0.8111	0.7976	0.8877
5000	0.05	0.7649	0.8194	0.8487
6000	0.041667	0.7757	0.8317	0.8667
8000	0.03125	0.7685	0.8083	0.8535
10000	0.025	0.708	0.8057	0.8641
11000	0.022727	0.6767	0.7493	0.8171

Table 4

Shear Stress Data (50% Duty Cycle)

		SHEAR STRESS		
Frequency	Pulse Width	1 kV	1.5 kV	2 kV
(Hz)	(ms)	(kPa)	(kPa)	(kPa)
100	5	0.9325	0.9507	1.0506
200	2.5	0.8748	0.9329	1.0227
500	1	0.8772	0.9686	1.02275
1000	0.5	0.8196	0.9032	1.0144
2000	0.25	0.8747	0.9386	0.99026
3000	0.166667	0.8203	0.9311	0.9599
4000	0.125	0.8171	0.872	0.9718
5000	0.1	0.7878	0.8397	0.9529
6000	0.083333	0.8202	0.8885	0.9926
8000	0.0625	0.7994	0.8403	0.9564
10000	0.05	0.7497	0.835	0.959
11000	0.045455	0.7479	0.7804	0.9423

Observations (Test 1A)

Figures 17, 18 and 19 show plots of shear stress vs frequency for duty cycles of 25%, 50% and 75% respectively.

1. Decrease in shear stress with increasing frequency: The ER effect decreases with increasing frequency at a constant field strength. At higher frequencies, the time available for charge transport between the two electrodes decreases and a fully

Table 5

Shear Stress Data (75% Duty Cycle)

		SHEAR STRESS		
Frequency	Pulse Width	1 kV	1.5 kV	2 kV
(Hz)	(ms)	(kPa)	(kPa)	(kPa)
100	7.5	0.9544	1.0007	1.1178
200	3.75	0.8809	0.9688	1.0453
500	1.5	0.9095	0.9775	1.0453
1000	0.75	0.8869	0.9195	1.0177
2000	0.375	0.9002	0.9494	1.0502
3000	0.25	0.8304	0.9361	1.006
4000	0.1875	0.8189	0.9264	1.0026
5000	0.15	0.798	0.8761	1.0119
6000	0.125	0.8263	0.9366	1.0233
8000	0.09375	0.8073	0.8891	0.9618
10000	0.075	0.7542	0.8818	0.9687
11000	0.068182	0.7556	0.7884	0.9627

polarized state cannot be achieved. For an increase in frequency from 100 to 11000 Hz, the shear stress for voltage of 1 kV decreases by 14.3%, 20% and 21%; for voltage of 1.5 kV decreases by 19%, 18% and 21.2%; and for voltage of 2 kV decreases by 20.7%, 10.3% and 13.8% for duty cycles of 25%, 50% and 75% respectively.

2. Increase in shear stress with increased field strength: The charge transport time required per unit distance is reduced at higher field strengths at a given

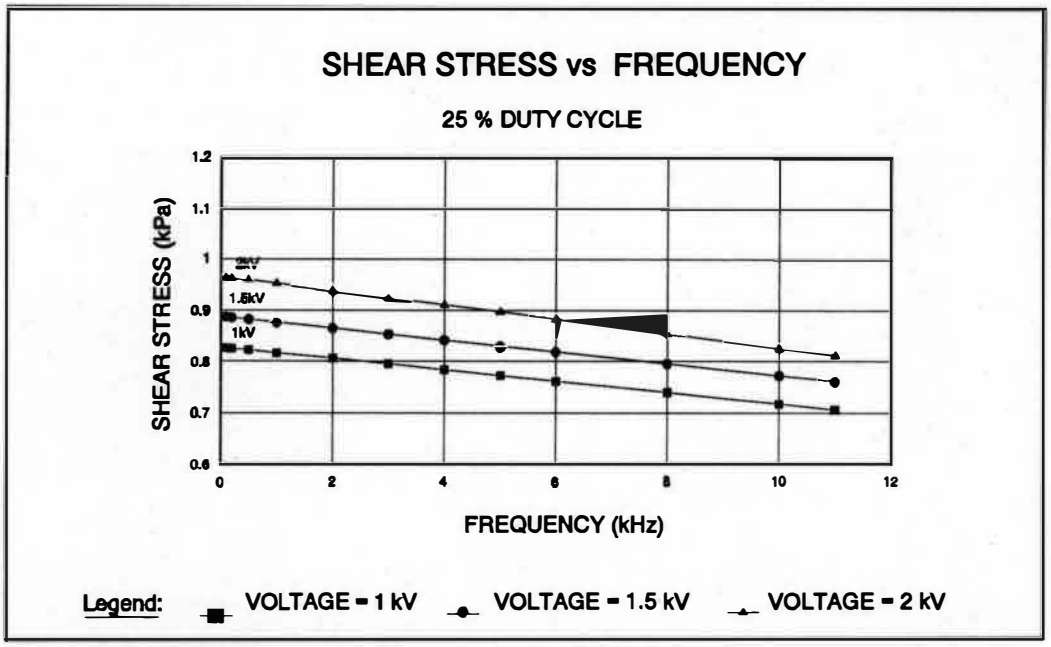

Figure 17. Shear Stress vs Frequency for 25% Duty Cycle.

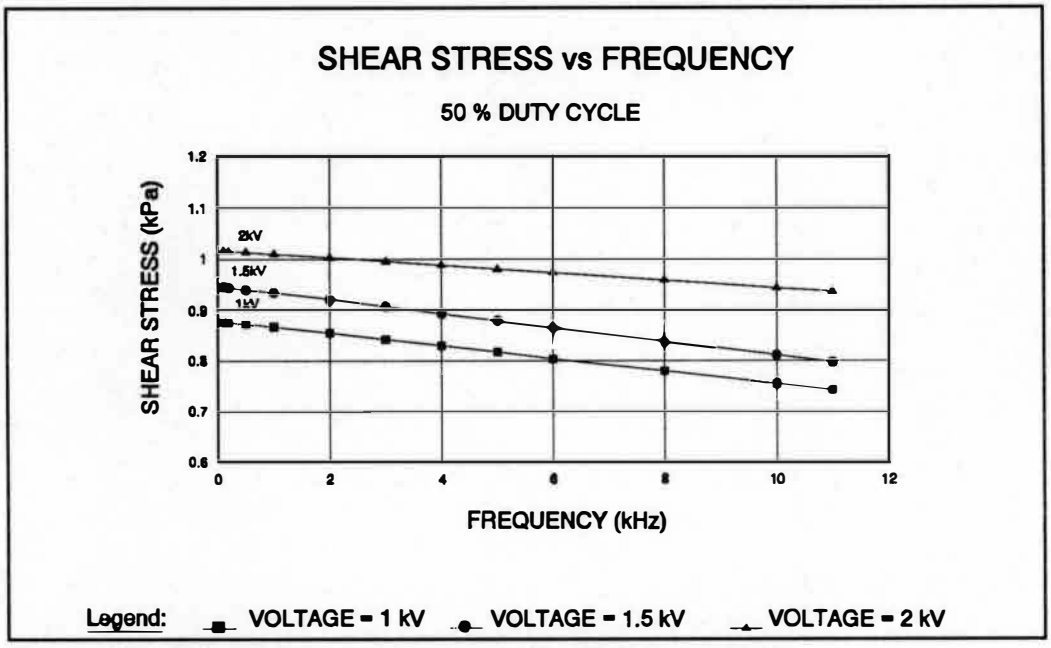

Figure 18. Shear Stress vs Frequency for 50% Duty Cycle.

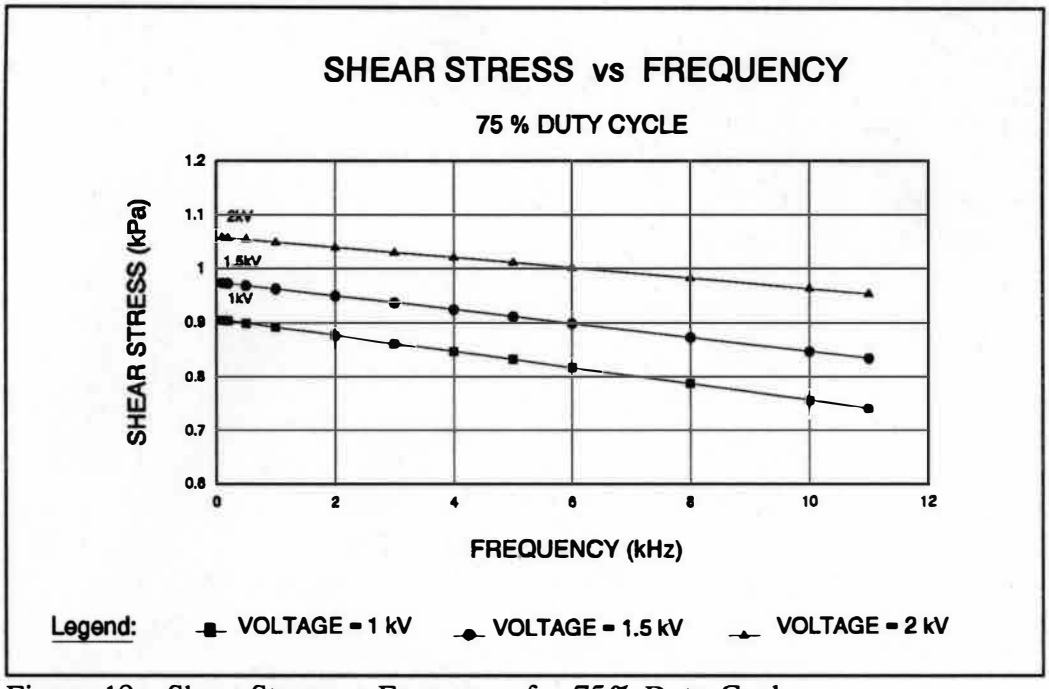

Figure 19. Shear Stress vs Frequency for 75% Duty Cycle.

frequency and thus ER effect increases.

At frequency of 100 Hz the shear stress increases by 30%, 12% and 17% for duty cycles of 25%, 50% and 75% respectively for a change in voltage from 1 kV to 2 kV.

At frequency of 11000 Hz the shear stress increases by 21%, 26% and 27% for duty cycles of 25%, 50% and 75% respectively for a change in voltage from 1 kV to 2 kV.

3. Increase in temperature by 4 ^{0}F: The temperature of the fluid within the open test cell was observed to increase by 4 ^{0}F during the period of intermittent experimentation (90 mins).

Objective (Test 1B)

The objective of this test was to determine the dependence of shear stress on frequency at different duty cycles. The electrode gap and speed were held at a constant value. The readings of shear stress were taken at variable frequency, voltage and duty cycles settings.

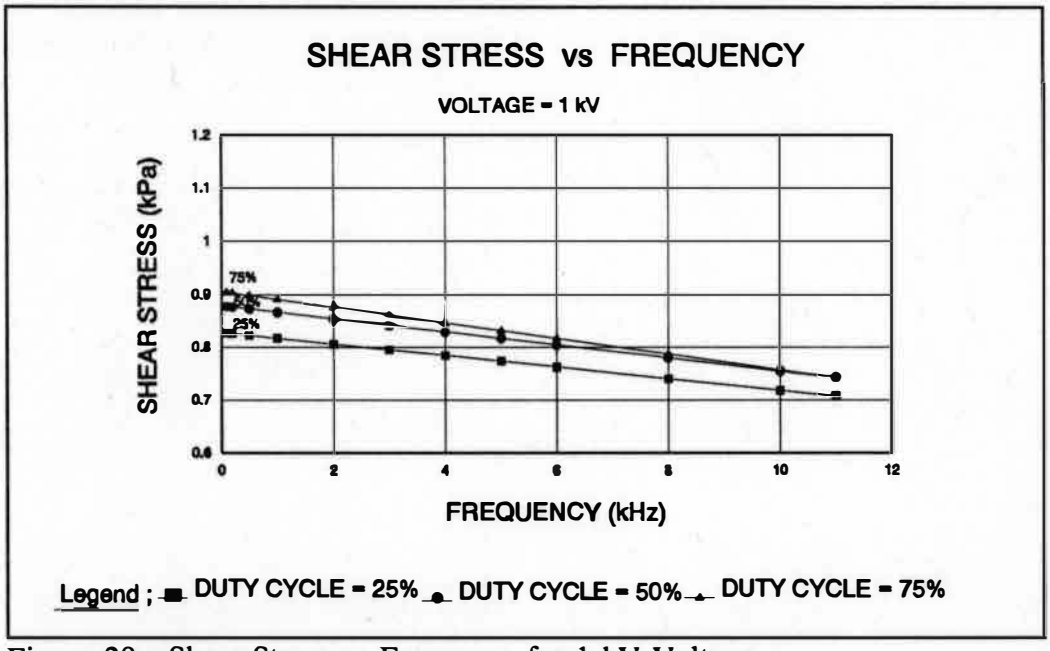

Figure 20. Shear Stress vs Frequency for 1 kV Voltage.

Observations (Test 1B)

Figures 20, 21 and 22 show plots of shear stress vs frequency for voltages of 1 kV, 1.5 kV and 2 kV respectively.

1. Increase in shear stress with increasing pulse-width: The shear stress and thus, the ER effect was observed to increase with increasing pulse-width at a constant

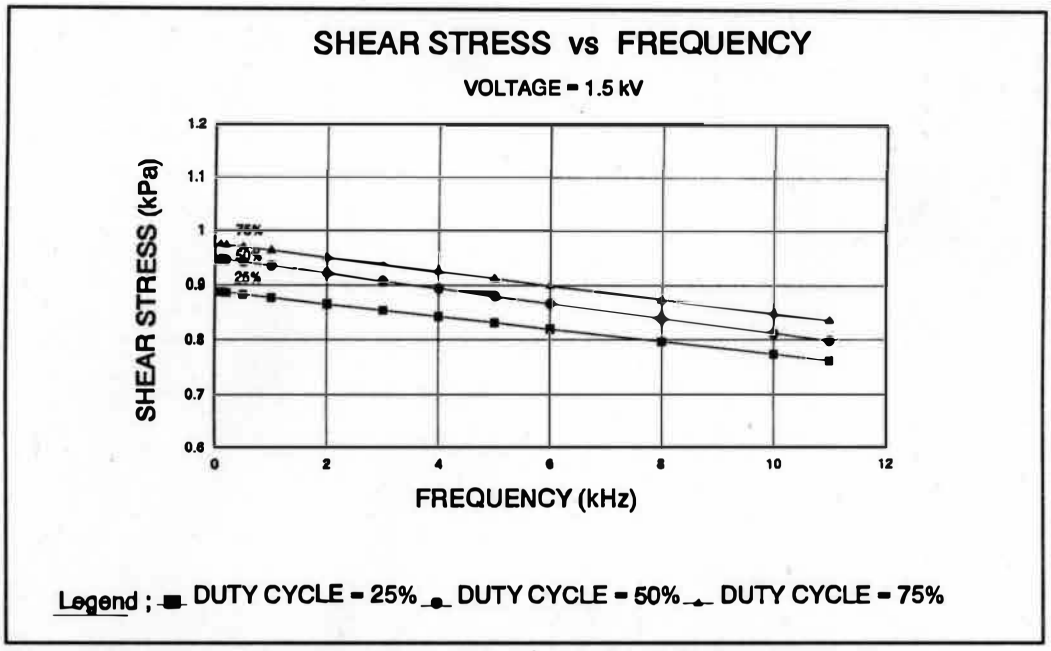

Figure 21. Shear Stress vs Frequency for 1.5 kV Voltage.

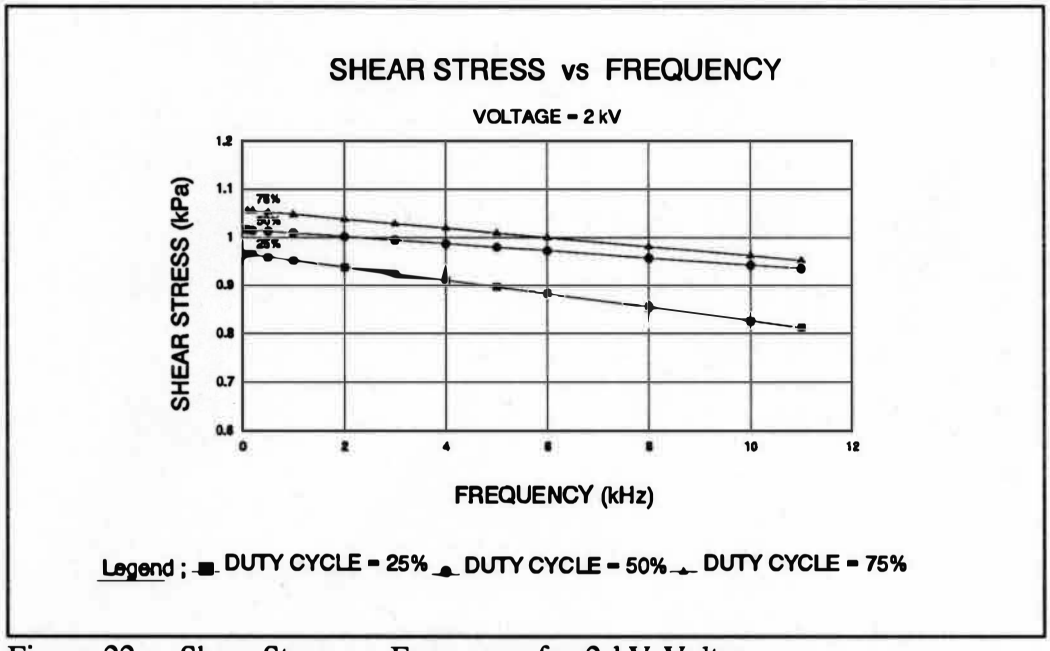

Figure 22. Shear Stress vs Frequency for 2 kV Voltage.

voltage because the electrical energization of the fluid occurs for a longer period of time. At a frequency of 100 Hz the shear stress increases by 20.7%, 8% and 8.5% for voltages of 1 kV, 1.5 kV and 2 kV respectively for a change in duty cycle from 25% to 75%. At frequency of 11000 Hz the shear stress increases by 11.6%, 5.2% and 17.8% for voltages of 1 kV, 1.5 kV and 2 kV respectively for a change in duty cycle from 25% to 75%.

3-D Shear Stress Surface Equations

The values of shear stress for different duty-cycles, frequencies and voltages are given in Table 6.

Table 6

Regressed Shear Stress (Function of Frequency)

Duty Cycle		X Coefficient(s)		
	Constant	Frequency	Voltage	R-Squared
25%	0.705499	-0.000012	0.126142	0.99373
50%	0.709114	-0.000012	0.159534	0.9738
75%	0.718713	-0.000012	0.174225	0.987

1. The value of the Constant shows a 1.8% increase from 25% to 75% duty cycle indicating an increase in shear stress with increasing duty cycle.

2. The value of Coefficient of Frequency is quite small and almost constant from 25% to 75% duty cycle, indicating that the coefficient of frequency has a small

effect on shear stress. It has a negative slope which causes the shear stress to decrease with increasing frequency.

3. The value of Coefficient of Voltage increases by 26% from 25% to 50% duty cycle and 9% from 50% to 75% duty cycle. Thus Voltage has a significant effect on shear stress for an increase in duty-cycle from 25% to 50%.

Figures 23, 24 and 25 show 3-D plots of shear stress vs frequency vs voltage for duty cycles of 25%, 50% and 75% respectively. These shear stress data were fit to the following equations:

$$SS_{25\%} = 0.705499 + Frequency*(-0.000012) + Voltage*(0.126142) \quad (8)$$

$$SS_{50\%} = 0.709114 + Frequency*(-0.000012) + Voltage*(0.159534) \quad (9)$$

$$SS_{75\%} = 0.718713 + Frequency*(-0.000012) + Voltage*(0.174225) \quad (10)$$

Example Calculations for Shear Stress as a Function of Frequency

To determine shear stress for 25% duty cycle, at a Frequency of 500 Hz and Voltage of 1.5 kV. Using the equation (8), we get:

$SS_{25\%} = 0.705499 + 500 * (-0.000012) + 1.5 * (0.126142)$

$SS_{25\%} = 0.888712$ kPa.

Comparing with the experimental data for 25% duty cycle, the shear stress at Frequency of 500 Hz and Voltage of 1.5 kV is:

$SS_e = 0.9146$ kPa.

Thus, the discrepancy between the value obtained from the equation and the value measured experimentally was 2%.

Shear Stress as a Function of Pulse-Width

The regressed values for combined duty-cycles, different pulse widths voltages are given in Table 7.

Table 7

Regressed Shear Stress (Function of Pulse-Width)

Duty Cycle		X Coefficient(s)			
25% - 75%	Constant	PWidth	Voltage	log(PW)	log(log (PW)^2)
	0.745173	-0.01705	0.1533	0.10437	0.00382

Observations (3-D Shear Stress Surface)

Figure 26 shows a 3-D graph of shear stress vs pulse-width vs voltage for a combined duty-cycle of 25%, 50% and 75%. The Constant, Voltage and Log(PWidth) have a significant effect on shear stress. The combined equation of shear stress as a function of pulse width for duty cycles of 25% to 75% is given by Equation 11.

$$SS = 0.74517 + PWidth*(-0.01705) + Voltage*(0.1533) + \log(PWidth)*(0.10437) + \log(\log(PWidth)^2)*(0.003826) \quad (11)$$

Example Calculations for Shear Stress as a Function of Pulse-Width (3-D Surface)

Shear stress from graph 26, at Pwidth of 5 ms and Voltage of 2 kV, can be obtained using the above equation:

SS = 0.745173 + 5 * (-0.01705) + 2 * (0.1533)

+ Log(5) *(0.10437) + Log(Log(5)^2) *(0.003826) = 1.04003 kPa.

From experimental data, shear stress (SS_e) with Pwidth of 5 ms and Voltage of 1.5 kV is 1.0506 kPa. Thus, the discrepancy between the value obtained from the equation and the value measured experimentally was 1%.

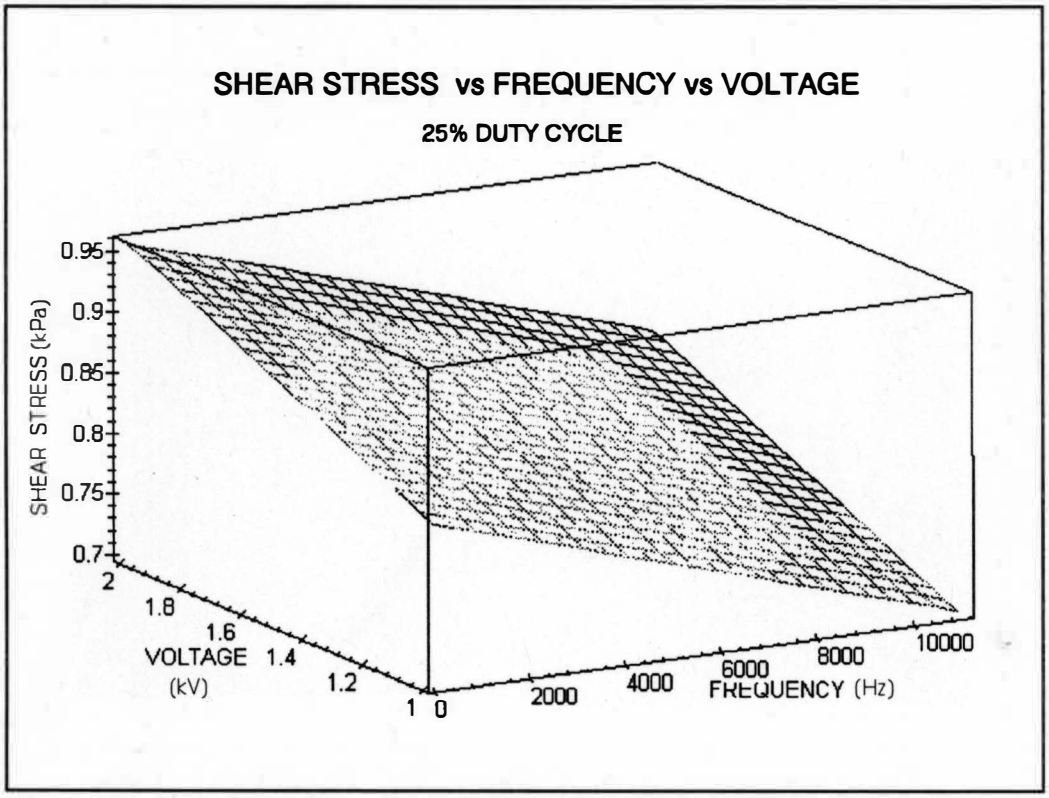

Figure 23. Shear Stress vs Frequency vs Voltage for 25% Duty Cycle.

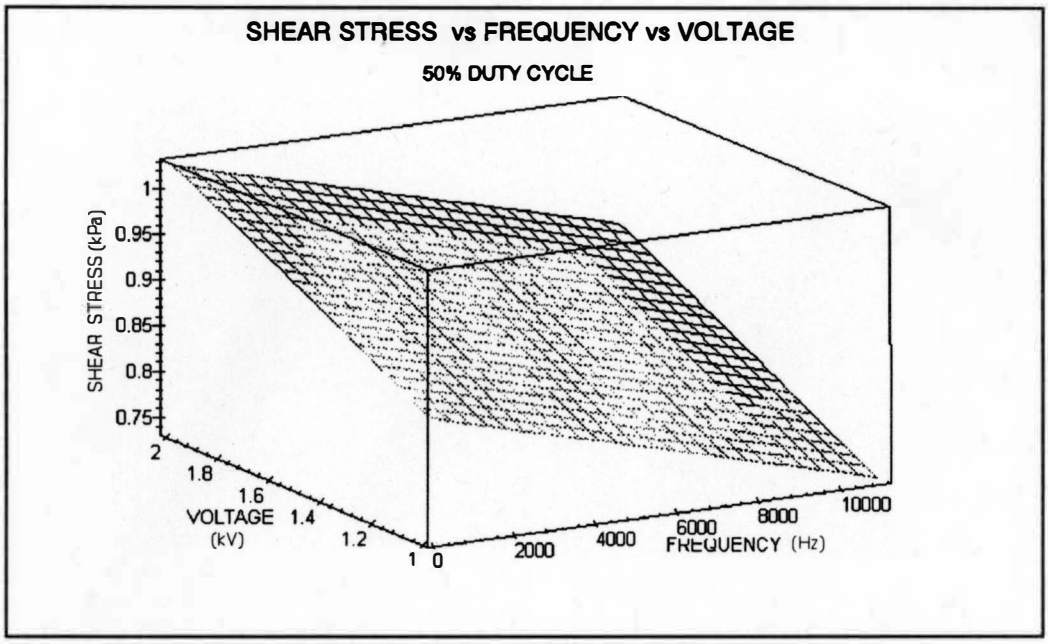

Figure 24. Shear Stress vs Frequency vs Voltage for 50% Duty Cycle.

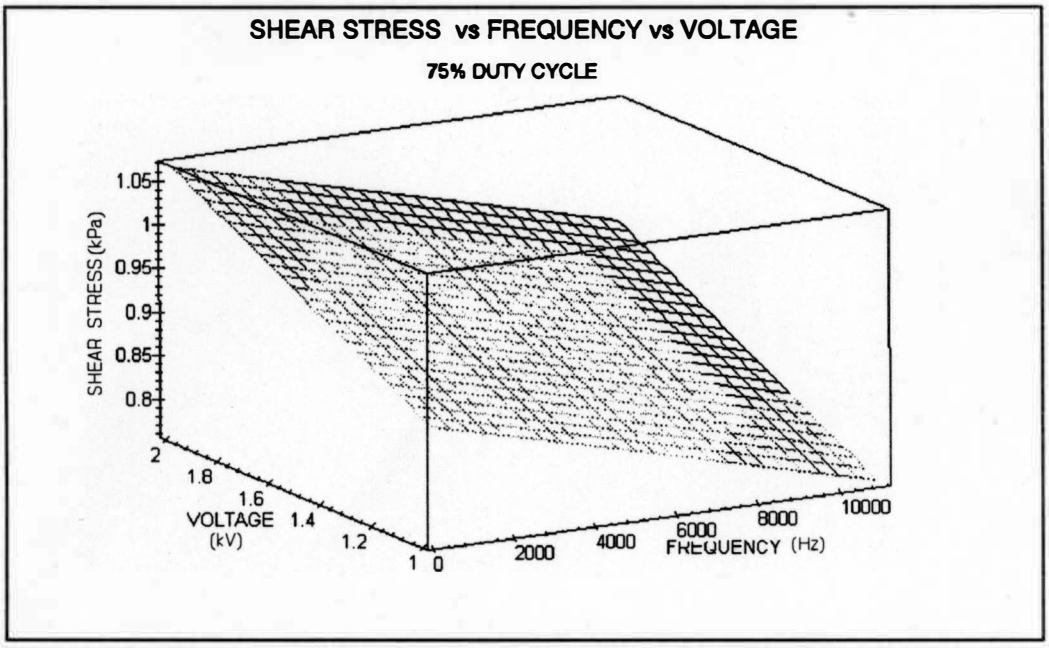

Figure 25. Shear Stress vs Frequency vs Voltage for 75% Duty Cycle.

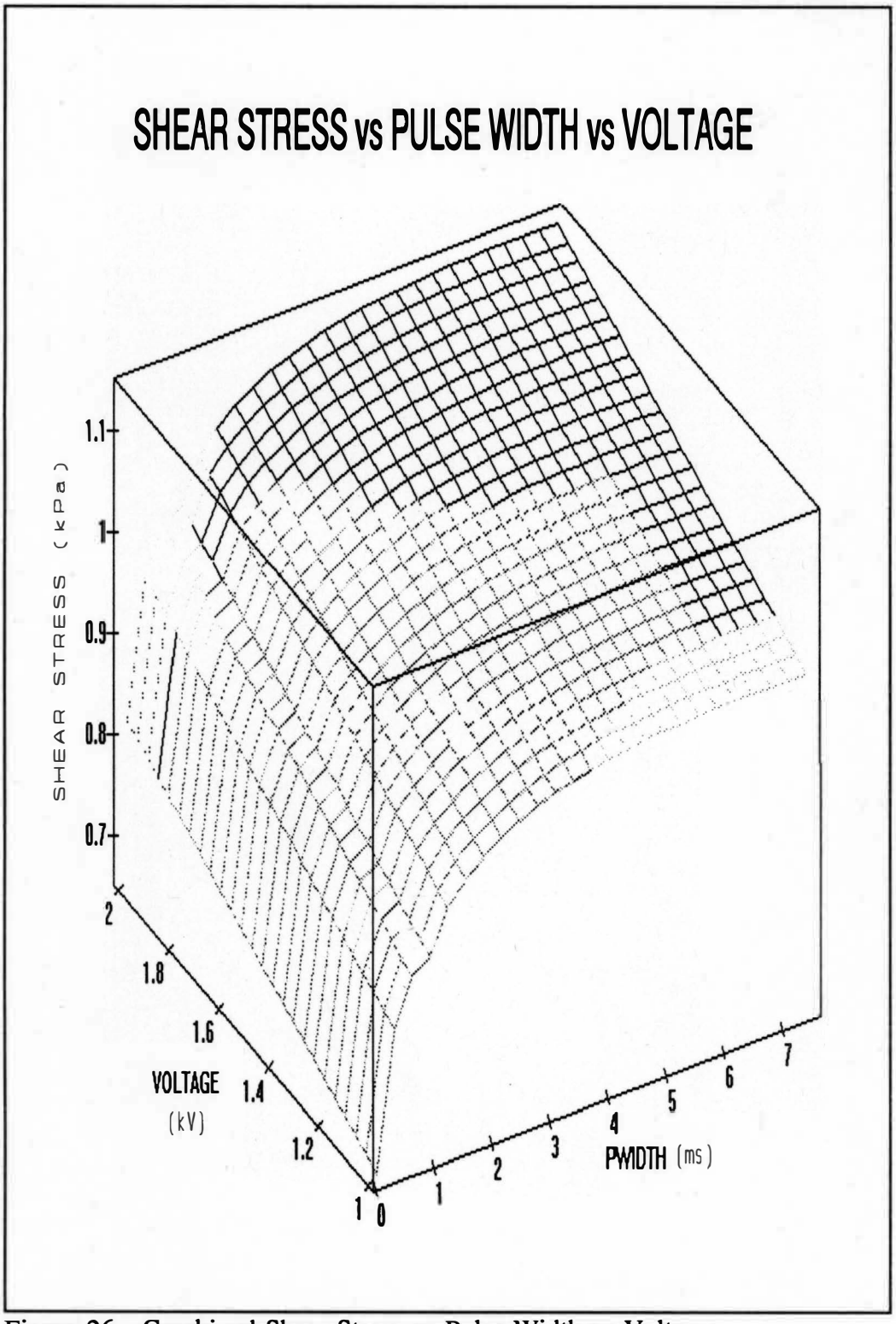

Figure 26. Combined Shear Stress vs Pulse Width vs Voltage.

Frequency at a particular duty cycle and pulse width can be obtained using Equation 12.

$$Frequency\ (Hz) = \frac{DutyCycle}{PulseWidth\ (ms)} * 1000 \qquad (12)$$

Example Calculations for Shear Stress as a Function of Frequency (3-D Surface)

The shear stress at pulse width of 5 ms, duty cycle of 50% and voltage of 2 kV can be calculated using equation for the combined shear stress. Using equation (11),

$$\mathbf{SS_{50\%} = 0.745173 + 5 * (-0.01705) + 2 * (0.1533) + Log(5) *(0.10437) + Log(Log(5)\hat{}2) *(0.003826)}$$

$$\mathbf{SS_{50\%} = 1.04003\ kPa.}$$

Shear stress as a function of frequency, can be determined using Equation 12 or by referring to Appendix B.

Frequency = 0.50/5 * 1000 = 100 Hz

Now, from equation (9) for shear stress for 50% Duty Cycle, at frequency of 100 Hz and Voltage of 1.5 kV, the shear stress can be obtained as:

$$\mathbf{SS_{50\%} = 0.709114 + 100 * (-0.000012) + 2 * (0.159534)}$$

$$\mathbf{SS_{50\%} = 1.026982\ kPa.}$$

Thus, the discrepancy between the value obtained from the equation and the value measured experimentally was 1%.

Test 2

Objective (Test 2A)

The objective of this test was to determine the dependence of electric power consumption on frequency at different voltages. The gap was held at a constant value. The readings of electric power consumption were taken at variable frequency, voltage and duty cycle settings.

Test Conditions

Table 8

Test Conditions (Test 2)

VOLTAGE	1, 1.5 and 2 kV
DUTY CYCLE	25%, 50% and 75%
FREQUENCY	100, 500, 1000, 5000 and 11000 Hz
GAP	0.04 in

Experimental Data

The Electric Power data for duty cycles of 25%, 50% and 75% is shown in Tables 9, 10 and 11 respectively.

Table 9

Electric Power Data (25% Duty Cycle)

	Power (milliWatts)	Power (milliWatts)	Power (milliWatts)
Frequency (Hz)	**1 kV**	**1.5 kV**	**2 kV**
100	0.817	0.9914	1.3571
500	0.851	1.094	1.39
1000	0.894	1.12	1.503
5000	1.2397	1.5545	1.899
11000	1.594	1.988	2.277

Table 10

Electric Power Data (50% Duty Cycle)

	Power (milliWatts)	Power (milliWatts)	Power (milliWatts)
Frequency (Hz)	**1 kV**	**1.5 kV**	**2 kV**
100	0.817	1.043	1.3998
500	0.852	1.145	1.457
1000	0.9	1.2277	1.59
5000	1.293	1.703	1.998
11000	1.631	2.096	2.453

Table 11

Electric Power Data (75% Duty Cycle)

	Power (milliWatts)	Power (milliWatts)	Power (milliWatts)
Frequency (Hz)	**1 kV**	**1.5 kV**	**2 kV**
100	0.831	1.1563	1.52
500	0.8712	1.206	1.595
1000	0.91	1.351	1.639
5000	1.32	1.867	2.094
11000	1.706	2.232	2.603

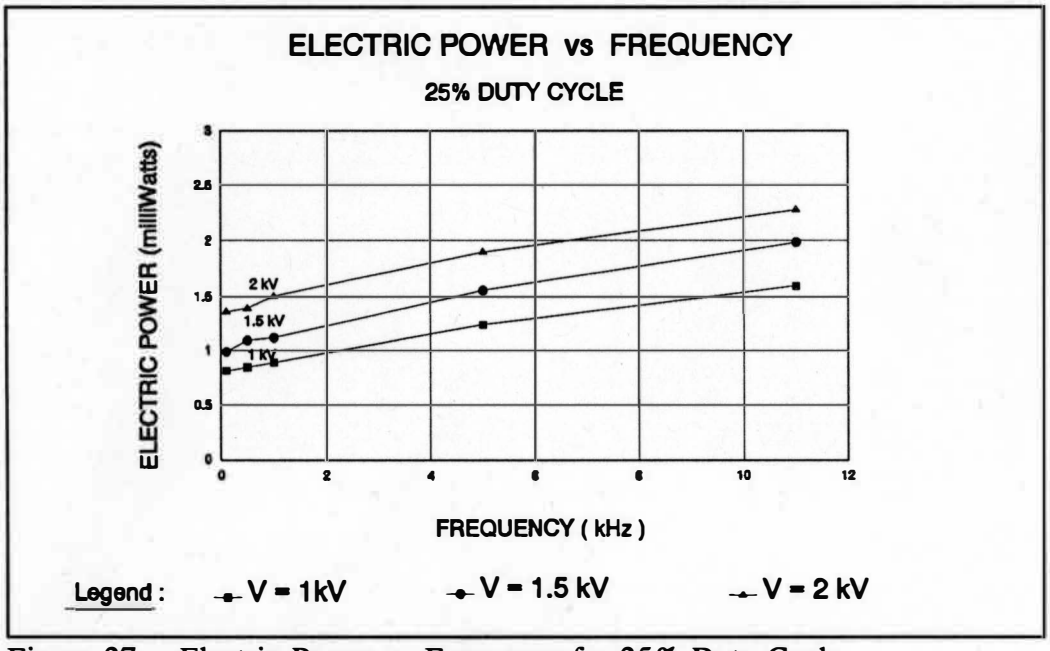

Figure 27. Electric Power vs Frequency for 25% Duty Cycle.

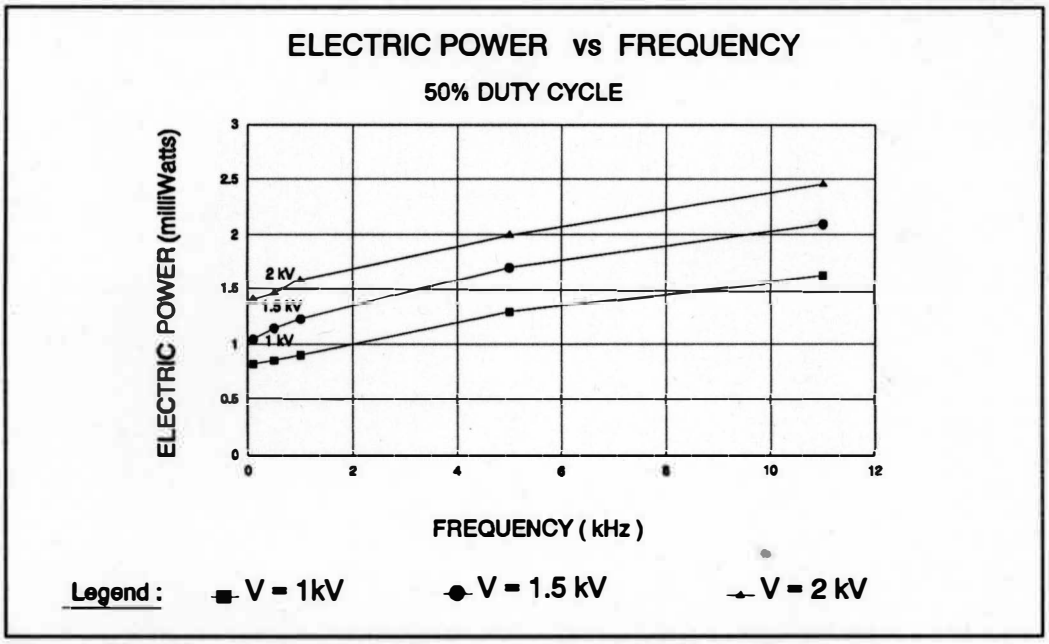

Figure 28. Electric Power vs Frequency for 50% Duty Cycle.

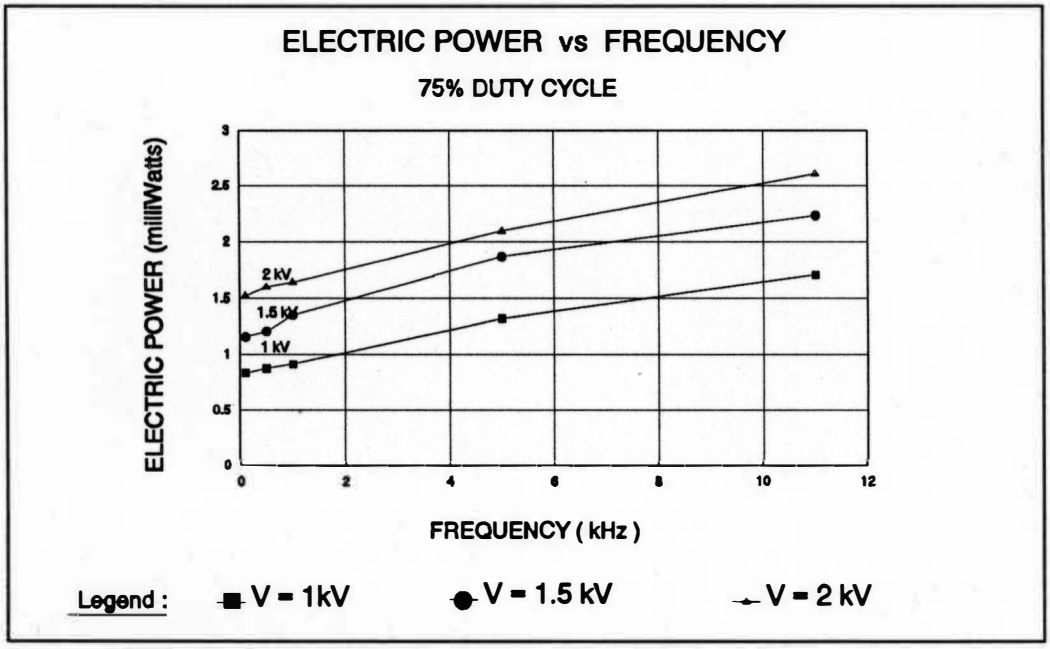

Figure 29. Electric Power vs Frequency for 75% Duty Cycle.

Observations (Test 2A)

Figures 27, 28 and 29 show plots of electric power vs frequency for duty cycles of 25%, 50% and 75% respectively.

1. Increase in power with increasing frequency: The power required by the ER fluid increases almost linearly with an increase in the AC frequency, thus exhibiting the properties similar to a capacitor. For an increase in frequency from 100 to 11000 Hz, the electric power for voltage of 1 kV increases by 95%, 99.6% and 105.3%; for voltage of 1.5 kV increases by 100%, 101% and 93%; and for voltage of 2 kV increases by 67.7%, 75% and 71% for duty cycles of 25%, 50% and 75% respectively.

2. Increase in Power with increasing voltage: The power required by the ER fluid is observed to exhibit an increase with increasing voltage.

At frequency of 100 Hz the power increases by 66%, 71% and 83% for duty cycles of 25%, 50% and 75% respectively for a change in voltage from 1 kV to 2 kV. At frequency of 11000 Hz the power increases by 43%, 50% and 52% for duty cycles of 25%, 50% and 75% respectively for a change in voltage from 1 kV to 2 kV.

Objective (Test 2B)

The objective of this test was to determine the dependence of electric power consumption on frequency at different duty-cycles. The gap was held at a constant

value. The readings of electric power consumption were taken at variable frequency, voltage and duty cycle settings.

Observations (Test 2B)

Figures 30, 31 and 32 show plots of electric power consumption vs frequency for voltages of 1 kV, 1.5 kV and 2 kV respectively.

1. Increase in Power with increasing pulse-width: The power required by the ER fluid is observed to exhibit an increase with increasing pulse-width. As the pulse-width increases the on-time of the cycle is more and thus more electric power is consumed.

At frequency of 100 Hz the power increases by 1.7%, 16.6% and 12% for

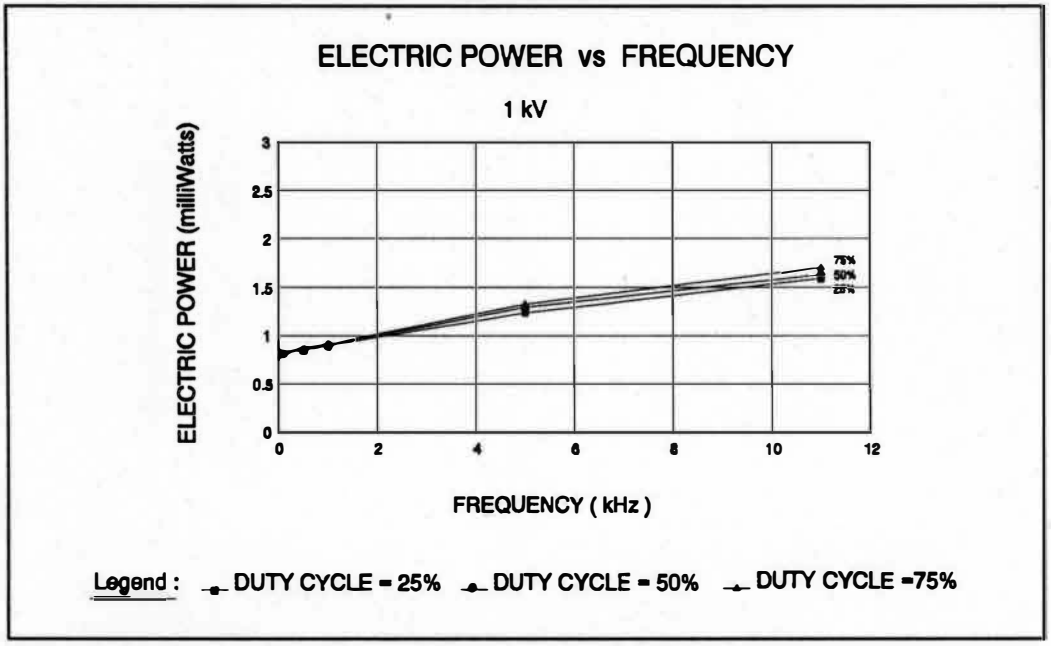

Figure 30. Electric Power vs Frequency for 1 kV Voltage.

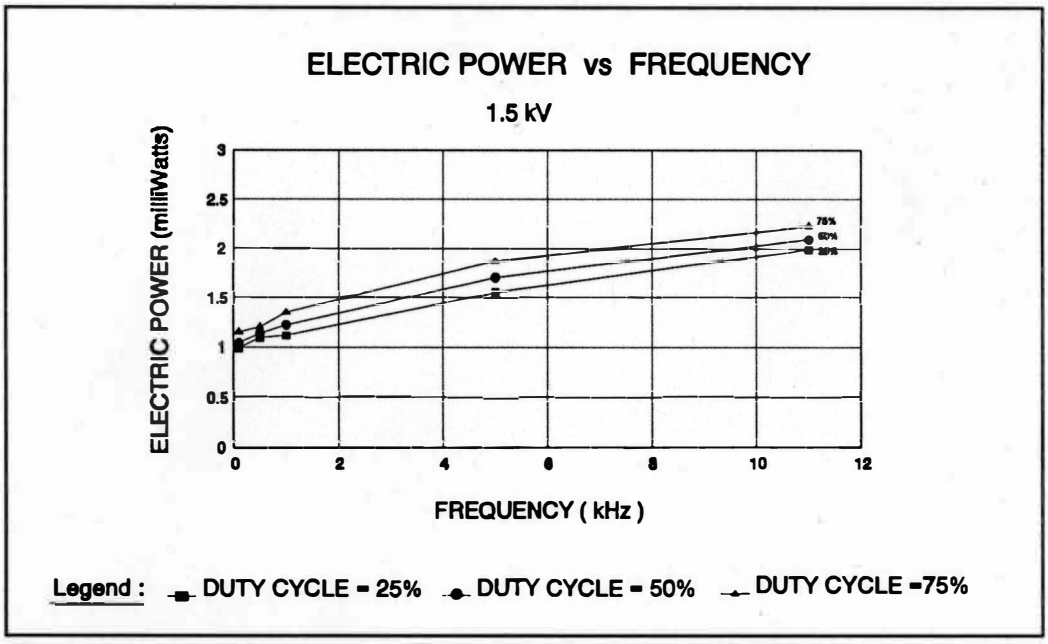

Figure 31. Electric Power vs Frequency for 1.5 kV Voltage.

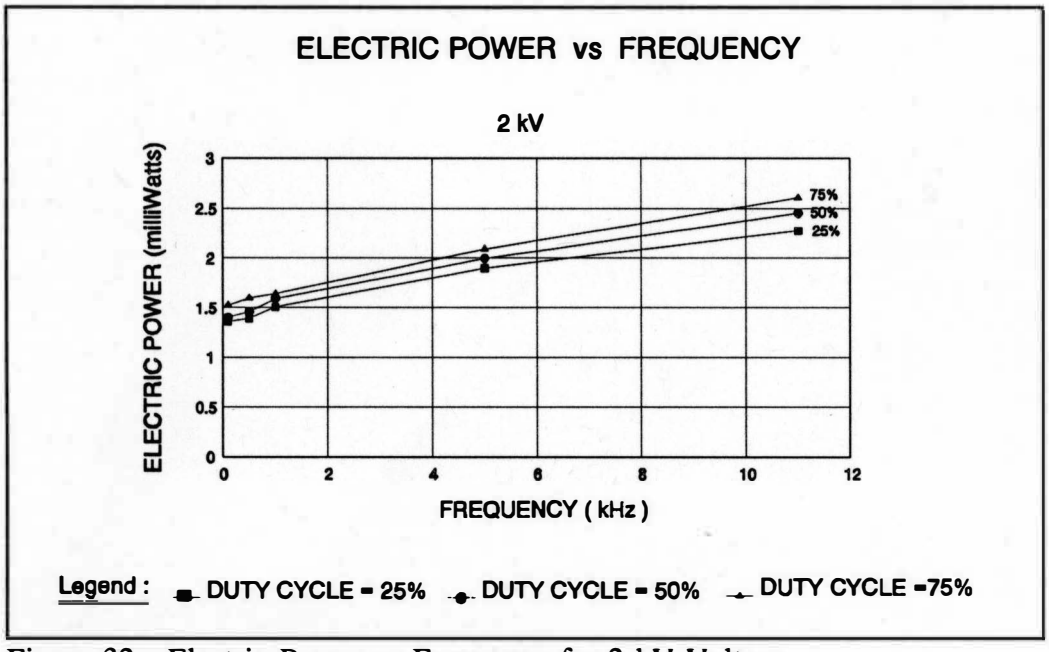

Figure 32. Electric Power vs Frequency for 2 kV Voltage.

voltages of 1 kV, 1.5 kV and 2 kV respectively for a change in duty cycle from 25%to 75%.

At frequency of 11000 Hz the power increases by 7%, 12.2% and 14.3% for voltages of 1 kV, 1.5 kV and 2 kV respectively for a change in duty cycle from 25% to 75%.

Test 3

The efficiency factor was found using Equation 13. Table 10 gives the equations for efficiency factor at duty cycles of 25%, 50% and 75% and voltages of 1 kV, 1.5 kV and 2 kV. The symbol FQ in Table 10 represents frequency in Hz.

$$Efficiency\ Factor = \frac{Shear\ Stress}{Power\ Input} \quad (kPa/mW) \tag{13}$$

Objective (Test 3A)

The objective of this test was to determine the dependence of efficiency factor on frequency at different voltages.

Experimental Data

The efficiency factor data for duty cycles of 25%, 50% and 75% is shown in Tables 13, 14 and 15 respectively.

Table 12

Efficiency Factor (kPa/mW) Calculation

Duty Cycle		**Efficiency Factor**	
	1 kV	**1.5 kV**	**2 kV**
25%	(-1.1E-5*FQ+.82) (.72E-4*FQ+.82)	(-1.2E-5*FQ+.88) (.9E-4*FQ+1.033)	(-1.4E-5*FQ+.97) (.89E-4*FQ+ 1.39)
50%	(-1.2E-5*FQ+.87) (.76E-4*FQ+.83)	(-1.4E-5*FQ+.94) (.95E-4*FQ+1.11)	(-7.4E-6*FQ+1.017) (.95E-4*FQ+ 1.44)
75%	(-1.5E-5*FQ+.91) (.81E-4*FQ+.84)	(-1.3E-5*FQ+.97) (.99E-4*FQ+1.21)	(-9.6E-6*FQ+1.058) (.99E-4*FQ+ 1.54)

Observations (Test 3A)

Figures 33, 34 and 35 show plots of efficiency factor vs frequency for duty cycles of 25%, 50% and 75% respectively.

1. Decrease in efficiency factor with increasing frequency: Shear stress was observed to increase and electric power was observed to decrease with increasing frequency. Thus, the ratio of shear stress to electric power decreases with increasing frequency. For an increase in frequency from 100 to 11000 Hz, efficiency factor for voltage of 1 kV decreases by 55.9%, 57% and 60%; for voltage of 1.5 kV decreases by 56%, 56.4% and 54.6%; and for voltage of 2 kV decreases by 49%, 45.6% and 46.8% for duty cycles of 25%, 50% and 75% respectively.

2. Decrease in efficiency factor with increasing voltage: The proportional increase of electric power with increasing voltage is higher than the increase in shear

Table 13

Efficiency Factor Data (25% Duty Cycle)

	Efficiency Factor (kPa/milliWatts)		
Frequency (Hz)	**1 kV**	**1.5 kV**	**2 kV**
100	0.993215	0.850845	0.691921
200	0.983394	0.842424	0.686736
500	0.954915	0.818002	0.671553
1000	0.910497	0.779906	0.647416
2000	0.831553	0.71219	0.603094
3000	0.763522	0.653822	0.56336
4000	0.704287	0.602992	0.527536
5000	0.652245	0.558329	0.495071
6000	0.606162	0.518774	0.465516
8000	0.528197	0.451844	0.413695
10000	0.464759	0.397374	0.369749
11000	0.437274	0.373773	0.350189

stress with increasing voltage. Thus, the ratio of shear stress to electric power decreases with increasing voltage at a particular frequency.

At frequency of 100 Hz the efficiency factor decreases by 30%, 33% and 36% for duty cycles of 25%, 50% and 75% respectively for a change in voltage from 1 kV to 2 kV.

At frequency of 1100 Hz the efficiency factor decreases by 20%, 16% and

Table 14

Efficiency Factor Data (50% Duty Cycle)

	Efficiency Factor (kPa/milliWatts)		
Frequency (Hz)	**1 kV**	**1.5 kV**	**2 kV**
100	1.047191	0.845808	0.69922
200	1.036371	0.837447	0.694176
500	1.005048	0.81319	0.679432
1000	0.95634	0.775311	0.656071
2000	0.870219	0.707861	0.613421
3000	0.796456	0.649601	0.575456
4000	0.732569	0.598772	0.541444
5000	0.676698	0.554038	0.510797
6000	0.627425	0.514365	0.483041
8000	0.544489	0.447114	0.434703
10000	0.477397	0.392271	0.394036
11000	0.448439	0.368477	0.37603

15% for duty cycles of 25%, 50% and 75% respectively for a change in voltage from 1 kV to 2 kV.

Objective (Test 3B)

The objective of this test was to determine the dependence of efficiency factor on frequency at different duty cycles. Efficiency factor was found from equation 13.

Table 15

Efficiency Factor Data (75% Duty Cycle)

	Efficiency Factor (kPa/milliWatts)		
Frequency (Hz)	**1 kV**	**1.5 kV**	**2 kV**
100	1.066353	0.795903	0.681036
200	1.054526	0.78846	0.676106
500	1.020349	0.766831	0.661685
1000	0.967391	0.732958	0.638809
2000	0.874306	0.672339	0.59696
3000	0.795133	0.619667	0.559616
4000	0.72697	0.573474	0.526086
5000	0.667669	0.532634	0.495814
6000	0.615609	0.496269	0.468347
8000	0.528481	0.434308	0.420402
10000	0.458452	0.383483	0.379954
11000	0.42835	0.361348	0.362012

Observations (Test 3B)

Figures 36, 37 and 38 show plots of efficiency factor vs frequency for voltages of 1 kV, 1.5 kV and 2 kV respectively.

1. Small change efficiency factor with duty cycle: The efficiency factor is observed to exhibit a slight change with a change in the duty cycle.

At frequency of 100 Hz the efficiency factor increases by 7.3% and decreases

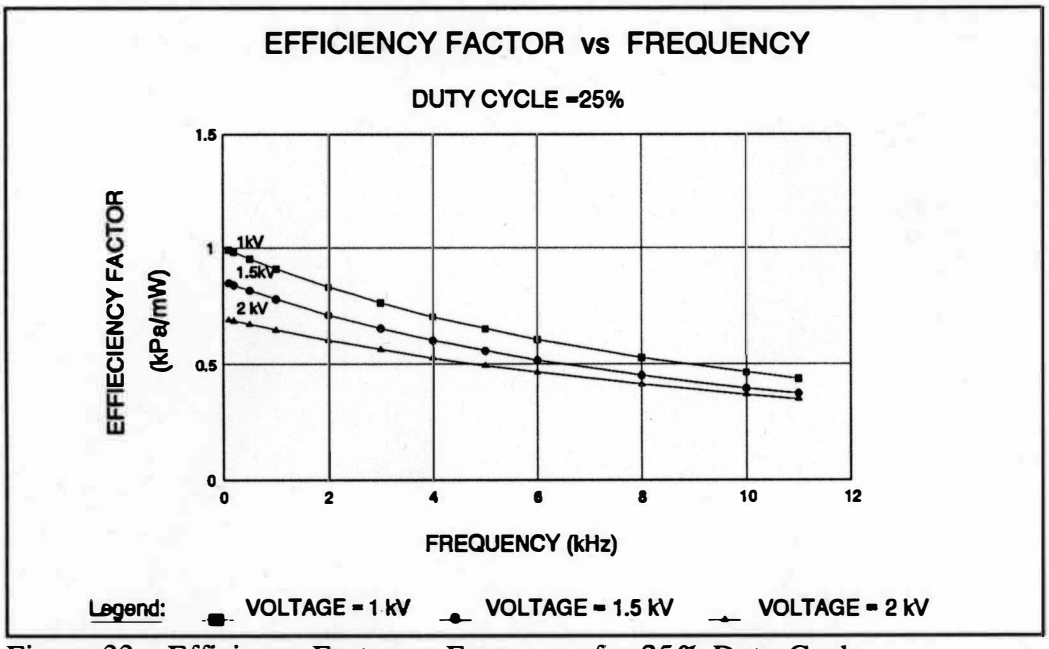

Figure 33. Efficiency Factor vs Frequency for 25% Duty Cycle.

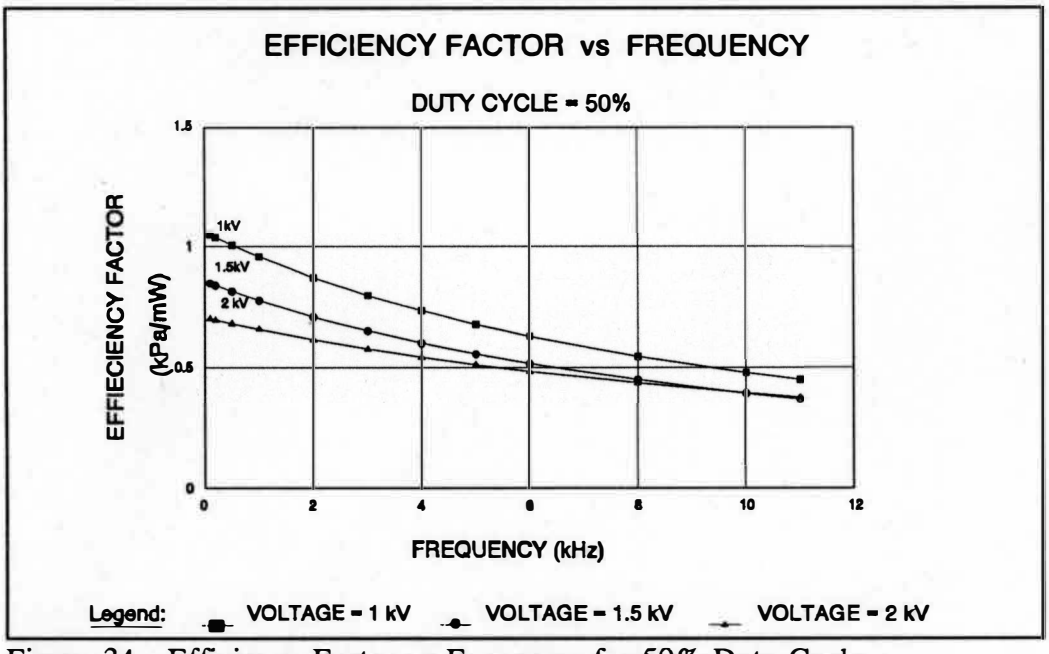

Figure 34. Efficiency Factor vs Frequency for 50% Duty Cycle.

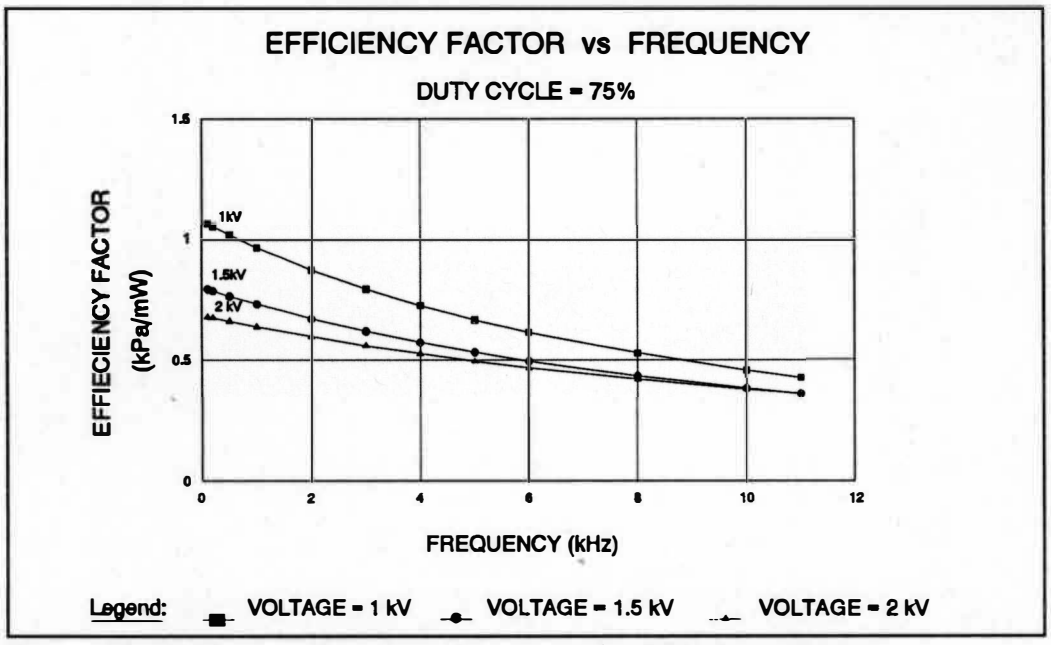

Figure 35. Efficiency Factor vs Frequency for 75% Duty Cycle.

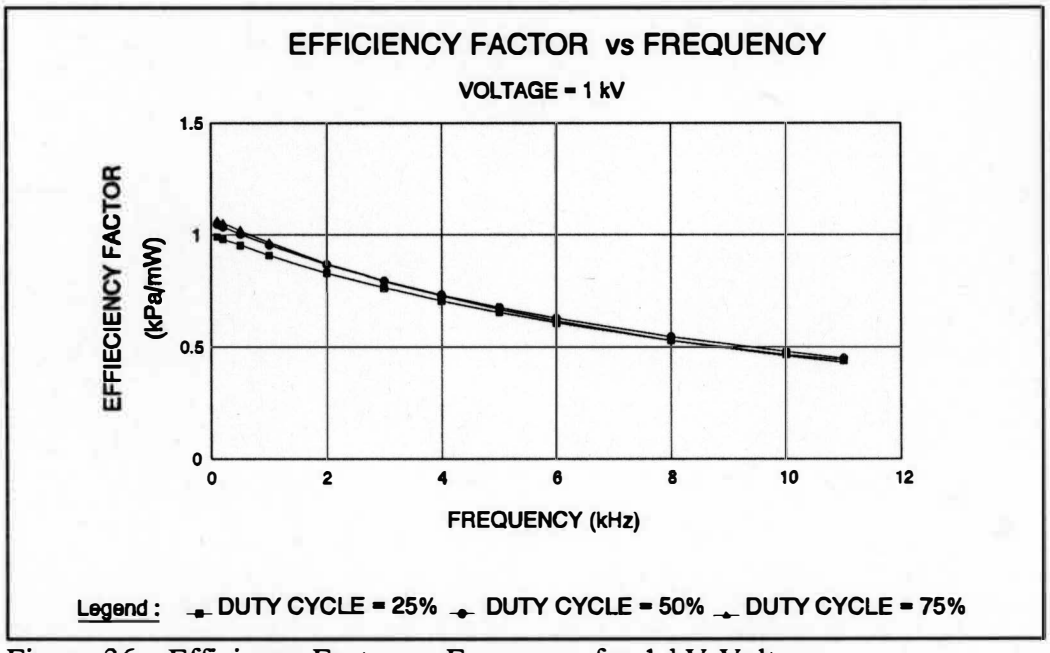

Figure 36. Efficiency Factor vs Frequency for 1 kV Voltage.

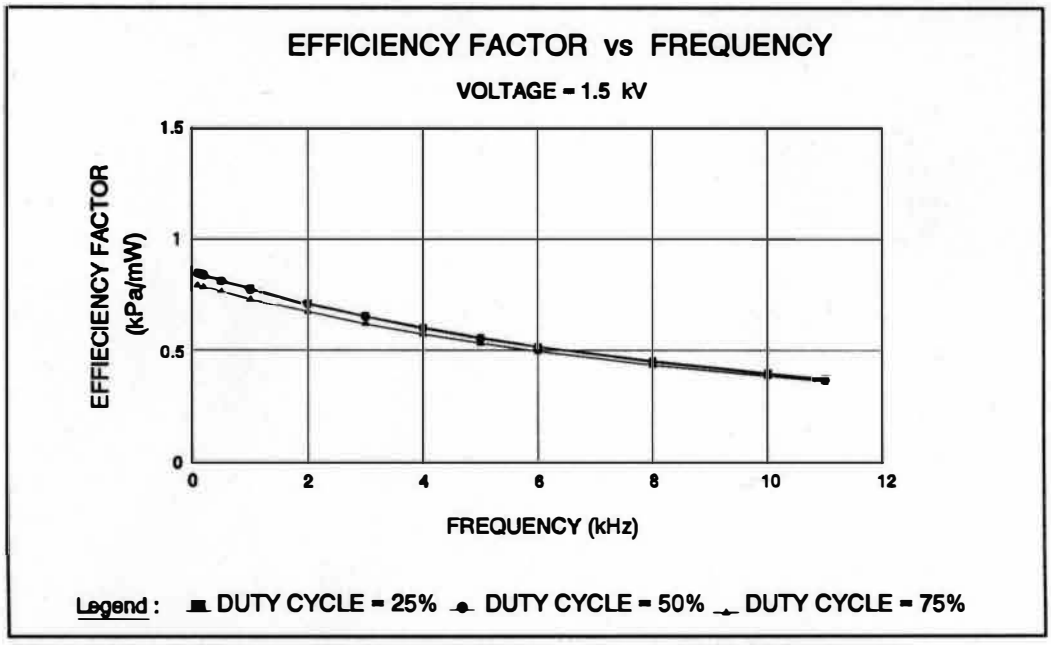

Figure 37. Efficiency Factor vs Frequency for 1.5 kV Voltage.

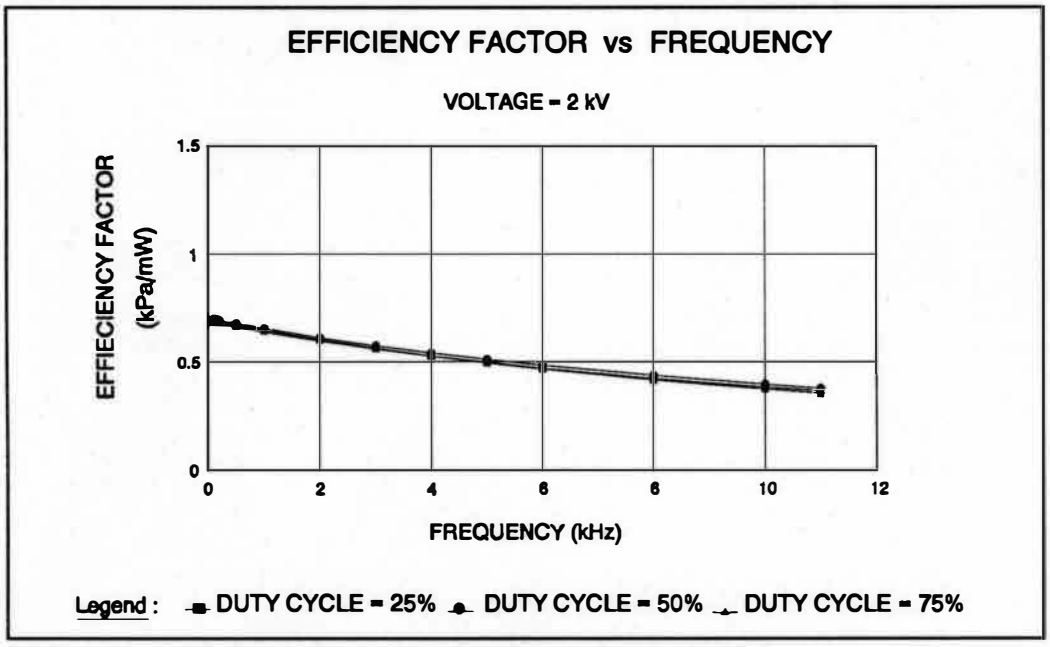

Figure 38. Efficiency Factor vs Frequency for 2 kV Voltage.

by 6.4% and 1.5% for voltages of 1 kV, 1.5 kV and 2 kV respectively for a change in duty cycle from 25% to 75%.

At frequency of 11000 Hz the efficiency factor decreases by 2%, 3.3% and increases by 3.4% for voltages of 1 kV, 1.5 kV and 2 kV respectively for a change in duty cycle from 25% to 75%.

3-D Efficiency Factor Surface Equations

The regressed values for different duty-cycles, frequencies and voltages are given in Table 16.

Table 16

Regressed Efficiency Factor (Function of Frequency)

Duty Cycle		**X Coefficient(s)**		
	Constant	**Frequency**	**Voltage**	**R-Squared**
25%	1.109078	-0.000043	-0.19535	0.947
50%	1.153376	-0.000043	-0.2134	0.925
75%	1.158982	-0.000043	-0.22806	0.902

1. The value of the Constant shows a 4.5% increase from 25% to 75% duty cycle.

2. The value of Coefficient of Frequency is constant from 25% to 75% duty cycle. It has a negative slope.

3. The value of Coefficient of Voltage decreases by 8.5% for an increase in duty-cycle from 25% to 50% and decreases by 6% for an increase in duty-cycle from 50% to 75%. Thus, it is observed that the decrease in efficiency factor with increasing voltage is slightly higher for an increase in duty-cycle from 25% to 50%.

4. Thus, the Constant and Voltage have a significant effect on efficiency factor.

Efficiency Factor can be determined by the following equations:

$$EF_{25\%} = 1.109078 + Frequency*(-0.000043) + Voltage*(-0.19535) \quad (14)$$

$$EF_{50\%} = 1.153376 + Frequency*(-0.000043) + Voltage*(-0.2134) \quad (15)$$

$$EF_{75\%} = 1.158982 + Frequency*(-0.000043) + Voltage*(-0.22806) \quad (16)$$

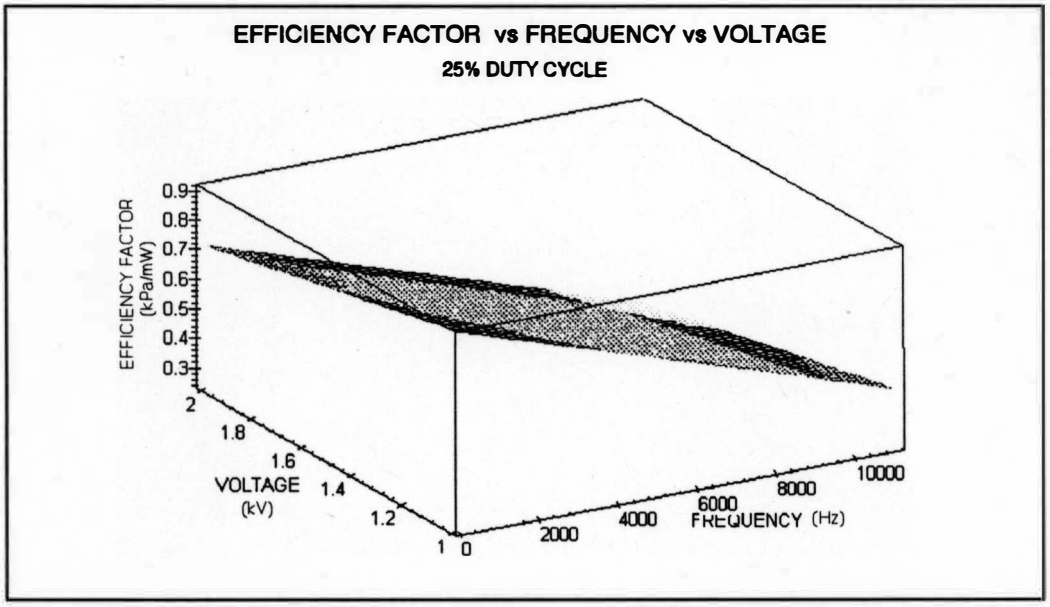

Figure 39. Efficiency Factor vs Frequency vs Voltage for 25% Duty Cycle.

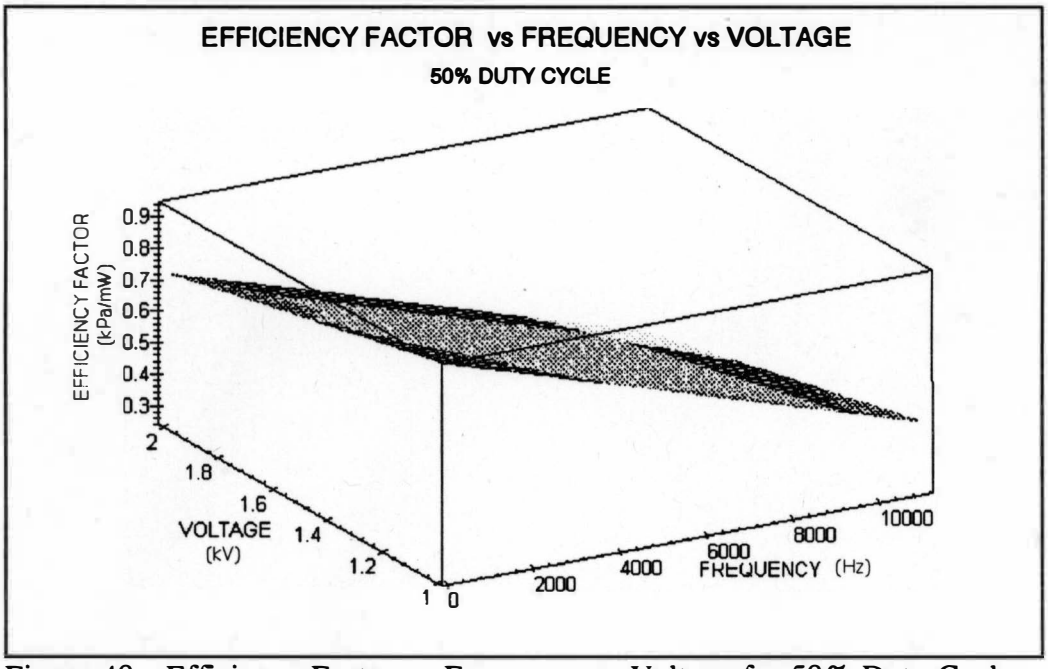

Figure 40. Efficiency Factor vs Frequency vs Voltage for 50% Duty Cycle.

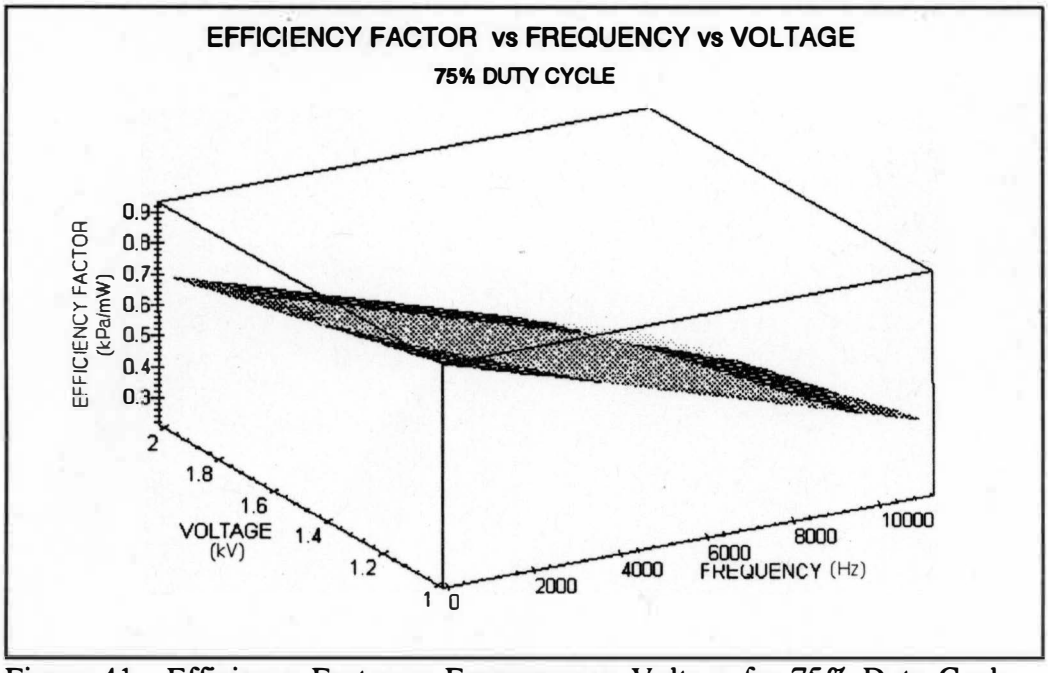

Figure 41. Efficiency Factor vs Frequency vs Voltage for 75% Duty Cycle.

Example Calculations for Efficiency Factor as a Function of Frequency

To determine efficiency factor for 75% duty cycle, at a Frequency of 100 Hz and Voltage of 2 kV, we use equation (16).

$EF_{75\%}$ = 1.158982 + 100 * (-0.000043) + 2 * (-0.22806)

$EF_{75\%}$ = 0.698562 kPa/milliWatts.

Comparing with the experimental data for 75% duty cycle, the efficiency factor at Frequency of 100 Hz and Voltage of 2 kV is:

EF_e = 0.681036 kPa/milliWatts.

Thus, the discrepancy between the value obtained from the equation and the value measured experimentally was 2%.

The regressed values for combined duty-cycles, different pulse widths voltages are given in Table 17.

Table 17

Regressed Efficiency Factor (Function of Pulse-Width)

Duty Cycle		**Coefficient(s)**			
25% - 75%	**Constant**	**PWidth**	**Voltage**	**log(PW)**	**log(log(PW)^2)**
	1.172997	-0.0379	-0.2122	0.28054	-0.0028

Observation (3-D Efficiency Factor Surface)

Figure 42 shows a 3-D graph of efficiency factor vs pulse-width vs voltage for a combined duty-cycle of 25%, 50% and 75%.

The Constant, Voltage and Log(PWidth) are observed to have a significant effect on efficiency factor.

The combined equation of efficiency factor as a function of pulse width for duty cycles of 25% to 75% is given by Equation 17.

$$EF = 1.172997 + PWidth*(-0.03792) + Voltage*(-0.2122) + \log(PWidth)*(0.28054) + \log(\log(PWidth)^2)*(-0.0028) \quad (17)$$

Example Calculations for Efficiency Factor as a Function of Pulse-Width (3-D Surface)

Efficiency factor from the combined graph, at Pwidth of 5 ms and Voltage of 1.5 kV, can be obtained using equation (17).

EF = 1.172997 + 5 * (-0.03792) + 1.5 * (-0.2122) + Log(5) *(0.28054)

+ Log(Log(5)^2) *(-0.0028) = **0.86025237 kPa/milliWatts.**

From the experimental data, efficiency factor with Pwidth of

5 ms and Voltage of 1.5 kV is:

EF_e = 0.845808 kPa/milliWatts.

Thus, the discrepancy between the value obtained from the equation and the value measured experimentally was 1%.

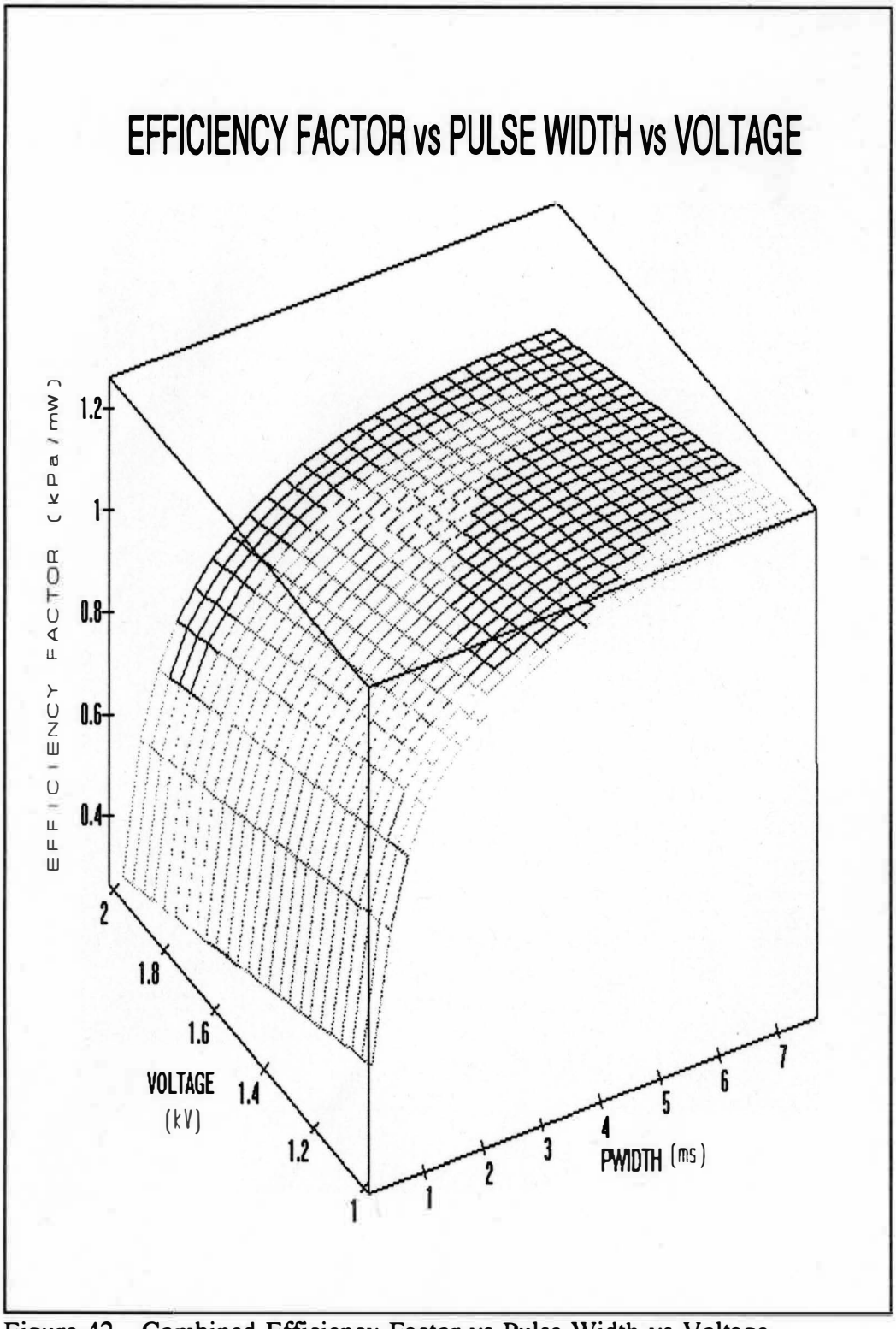

Figure 42. Combined Efficiency Factor vs Pulse Width vs Voltage.

Efficiency factor at a particular duty cycle, pulse width and voltage as a function of frequency, can be obtained using Equation 18 or by referring to Appendix B.

$$Frequency\ (Hz) = \frac{DutyCycle}{PulseWidth\ (ms)} * 1000 \qquad (18)$$

Example Calculations for Efficiency Factor as a Function of Frequency (3-D Surface)

From equation (17), the efficiency factor at pulse width of 5 ms, duty cycle of 50% and voltage of 1.5 kV is:

$EF_{50\%}$ = 1.172997 + 5 * (-0.03792) + 1.5 * (-0.2122) + Log(5) *(0.28054) + Log(Log(5)^2) *(-0.0028) = 0.860252 kPa/milliWatts.

To obtain efficiency factor as a function of frequency, we can determine frequency using equation (18) as:

Frequency = 0.50/5 * 1000 = 100 Hz

Now, from equation (15) the efficiency factor for 50% duty cycle, at frequency of 100 Hz and Voltage of 1.5 kV, can be obtained as:

$EF_{50\%}$ = 1.153376 + 100 * (-0.000043) + 1.5 * (-0.2134)

$EF_{50\%}$ = 0.828976 kPa/milliWatts.

Thus, the discrepancy between the value obtained from the equation and the value measured experimentally was 3%.

CHAPTER VII

CONCLUSION

Electrorheological (ER) Fluids are fluids whose physical properties can be altered in the presence of an electric field. The applications of ER fluids are presently limited by the impediments of high electric fields, increase in temperature and a lack of understanding of the effect of electric waveform on ER fluids.

The present research focused on the investigation of the dependence of electric waveform and frequency response of ER suspensions on the electric field by employing frequency and pulse-width modulation. The experiments were carried out at voltages of 1, 1.5 and 2 kV, frequencies ranging from 100 to 11000 Hz, pulse-widths ranging from 0.02 to 7.5 milliseconds and duty- cycles of 25%, 50% and 75% for a particular ER fluid which was responsive to an A.C. electric field only. The results obtained depended on the properties of a particular ER fluid test sample and on the stability of the instrumentation, power source and the pulser employed. The results obtained may or may not be true for test conditions other than those considered and for other ER fluids/samples. The University and all those involved in this research make no claim that the results obtained are completely error-free or comprehensive in all respects. The shear stress was observed to increase with increasing field strength and showed a drop with increasing frequency. The

efficiency factor was observed to drop with increasing frequency and voltage. Equations were developed for shear stress and efficiency factor as a function of frequency, duty cycle, voltage and pulse-width. The major factors affecting shear stress and efficiency factor were voltage and pulse-width.

From the equations of shear stress, for an increase in duty-cycle from 25% to 50% and 50% to 75%, it was observed that the change in shear stress with increasing voltage is more significant for an increase in duty-cycle from 25% to 50%.

From the equations of efficiency factor, for an increase in duty-cycle from 25% to 50%, and 50% to 75%, it was observed that the decrease in efficiency factor with increasing voltage is slightly higher for an increase in duty-cycle from 25% to 50%.

Under the experimental conditions, the maximum shear stress and the maximum efficiency factor were observed at voltages of 2 kV and 1 kV respectively, both occurring at a pulse-width of 7.5 ms and a frequency of 100 Hz, that is, at 75% duty cycle. At a voltage of 1 kV, the efficiency factor increases by 56.5% for a decrease in shear stress of 14.6%. Thus, selection of the most efficient operating range of ER fluids requires a trade-off.

This fundamental research will lead to the investigation of applications of ER fluids at WMU.

Appendix A

QuickBasic Software for Collecting and Plotting Data

QUICKBASIC SOFTWARE FOR COLLECTING AND PLOTTING DATA

```
'xxxxxxxxxxxxxxxxxxxxxxxxxxxxxxxxxxxxxxxxxxxxxxxxxxxxxxxxxxxxxxxxxxxxxxxxxxxxxxx
'            SHEAR STRESS,  SHEAR STRAIN & TEMPERATURE
'xxxxxxxxxxxxxxxxxxxxxxxxxxxxxxxxxxxxxxxxxxxxxxxxxxxxxxxxxxxxxxxxxxxxxxxxxxxxxxx

counter% = 1500
SCREEN 9
COLOR 1, 3
LOCATE 10, 20
INPUT "ENTER DATA FILE NAME"; MYFILE$
OPEN "O", #1, "c:\erf\" + MYFILE$ + ".DAT"
GAP = .04
CLS
LOCATE 10, 20
PRINT "PRESS ' Z' ONCE TO REMOVE OFFSET"
SLEEP (1)
CLS
WINDOW (0, 0)-(500, 4095)

npavg = 1500
npavg = npavg / 5
DIM stressint(npavg)
DIM strainint(npavg)
DIM tempint(npavg)


BADR = &H218                'set BASE address
OUT BADR, &H0               'INITIALIZE BOARD
OUT BADR, &H0               'write MODE 0 to CSR

BADR2 = BADR + 2
BADR3 = BADR + 3

LOCATE 25, 60
PRINT "FILE :-- "; MYFILE$
```

```
'-------------------------------------------------------------------------------
'                    READ THE CHANNELS
'-------------------------------------------------------------------------------
DO
j = j + 1
IF j > npavg THEN j = 1

    gcr = 128 + 64              '  READ CH-0 : STRESS: GAIN-8
    gcr = 0
    OUT BADR + 1, gcr
    WHILE INP(BADR) < 128: WEND
    STRESSDATASUM = STRESSDATASUM - stressint(j)
    STUM = STUM - stressint(j)
    stressint(j) = INP(BADR2) + 256 * INP(BADR3)
    STUM = STUM + stressint(j)
    IF (ABS(stressint(j) - stal) > 5) AND (stal < > 0) THEN
    stressint(j) = stal
    END IF

    STRESSDATASUM = STRESSDATASUM + stressint(j)

    gcr = 1                     '  READ CH-1: STRAIN: GAIN-1
    OUT BADR + 1, gcr
    WHILE INP(BADR) < 128: WEND

    STRAINDATASUM = STRAINDATASUM - strainint(j)
    strainint(j) = INP(BADR2) + 256 * INP(BADR3)
    STRAINDATASUM = STRAINDATASUM + strainint(j)

    gcr = 2                     '  READ CH-2: TEMPERATURE: GAIN-1
    OUT BADR + 1, gcr
    WHILE INP(BADR) < 128: WEND

    TEMPDATASUM = TEMPDATASUM - tempint(j)
    tempint(j) = INP(BADR2) + 256 * INP(BADR3)
    TEMPDATASUM = TEMPDATASUM + tempint(j)

Y = Y + 1
IF Y >= 50 THEN
LOCATE 1, 1

PRINT USING "STRAININT(J)--#####.##          STRESSINT(J)--#####.##
TEMPINT(J)--#####.##"; strainint(j); stressint(j); tempint(j)
```

```
Y = 0
END IF

IF A$ = CHR$(32) THEN counter% = 0:  'SPACE BAR TO STORE VALUES
 GOSUB ASOUND
  GOSUB CALIBRATE
   IF A$ = CHR$(90) THEN GOSUB ZERO              'TO REMOVE OFFSET
  GOSUB PLOT
LOOP

'-------------------------------------------------------------------------------------------
'                    CALIBRATION
'-------------------------------------------------------------------------------------------
CALIBRATE:
    stal = (STUM) / npavg
    Stressval = (STRESSDATASUM) / npavg
    Strainval = STRAINDATASUM / npavg
    TEMPVAL = TEMPDATASUM / npavg
'   STRESS
       T = .000104 * Stressval + .002353     'PRELOAD SPRING
       s = 156706.8 * T                      'SS=T/(A* Rm)
       SS = s / 1000 - SSI                   'SHEAR STRESS IN kPa

'    STRAIN
     RPM = .203824 * Strainval - 14.8407       ' GAP: 0.04"
     SHEARRATE = (RPM / 60 * .91672) / (GAP)

'    TEMPERATURE
     Tc = TEMPVAL * 1.150898 - 35.772
     Tf = 1.8 * Tc + 32
A$ = UCASE$(INKEY$)
IF A$ = CHR$(27) THEN
PRINT #1,
PRINT #1, "FILENAME:  "; MYFILE$
PRINT #1, "GAP     :  "; GAP
CLOSE 1: END
END IF
RETURN

'-------------------------------------------------------------------------------------------
'                      PLOT
'-------------------------------------------------------------------------------------------
PLOT:
```

```
   i = i + 1
   IF i >= 420 THEN i = 0: CLS
PSET (i, SS * 20), 15
LINE (i - 1, last * 2)-(i, stressint(j) * 2), 14
last = stressint(j)
PSET (i, SHEARRATE * 5), 5
PSET (i, Tc * 50), 8
RETURN

'-------------------------------------------------------------------------------------------
'                          SOUND & STORE
'-------------------------------------------------------------------------------------------
ASOUND:
counter% = counter% + 1
IF counter% > 32000 THEN counter% = 1500   '***prevent overflow

IF counter% = npavg THEN
  GOSUB CALIBRATE
  FOR SN = 440 TO 1000 STEP 10
  SOUND SN, SN / 10000
  NEXT SN
  GOSUB STORE
  GOSUB PRINTSCR
END IF
RETURN
'-------------------------------------------------------------------------------------------
'                          STORE
'-------------------------------------------------------------------------------------------
STORE:
PRINT #1, SHEARRATE, SS  ', Tc              'SHEARRATE: X-axis; SS: Y-axis

RETURN
```

```
' ------------------------------------------------------------------------------------------
'                              OUTPUT
' ------------------------------------------------------------------------------------------
PRINTSCR:
LOCATE 1, 1
PRINT "-  SHEAR RATE  -    - SHEAR STRESS -    -  TEMPERATURE - "

LOCATE 3, 1
PRINT USING "SHRATEVAL --#####.#### STRESSVAL--######.#### TEMPVAL
--#####.###"; Strainval; Stressval; TEMPVAL

LOCATE 5, 1
PRINT USING "SPEED--#####.#### rpm TORQUE--######.#### N-m Tc--#####.###
deg C";  RPM; T; Tc

LOCATE 7, 1
PRINT USING "SH RATE--#####.#### 1/s       SH STRESS--####.#### kPa
Tf--#####.### deg F"; SHEARRATE; SS; Tf

LOCATE 25, 1
INPUT "Press return to continue"; b$
IF b$ < > CHR$(9) THEN CLS
RETURN


'------------------------------------------------------------------------------------------
'                              ZERO OFFSET
'------------------------------------------------------------------------------------------
ZERO:
StressvalI = (STRESSDATASUM) / npavg
TI = .000104 * StressvalI + .002353     'PRELOAD SPRING

sI = 2 * 78353.4 * TI                    'SS=T/(A* Rm)
SSI = sI / 1000                         'SHEAR STRESS IN kPa
RETURN
```

Appendix B

Frequency to Pulse-Width Conversion Table

Frequency to Pulse-Width Conversion Table

FREQ	PULSE WIDTH (ms)		
(Hz)		Duty Cycle	
	25%	50%	75%
0	0.00	0.00	0.00
30	8.33	16.67	25.00
50	5.00	10.00	15.00
100	2.50	5.00	7.50
200	1.25	2.50	3.75
300	0.83	1.67	2.50
400	0.63	1.25	1.88
500	0.50	1.00	1.50
1000	0.25	0.50	0.75
2000	0.13	0.25	0.38
3000	0.08	0.17	0.25
4000	0.06	0.13	0.19
5000	0.05	0.10	0.15
6000	0.04	0.08	0.13
7000	0.04	0.07	0.11
8000	0.03	0.06	0.09
9000	0.03	0.06	0.08
10000	0.03	0.05	0.08
11000	0.02	0.05	0.07

Appendix C

Problems Encountered in Instrumentation

The major problem encountered in instrumentation was that of the noise and electromagnetic waves from the power source and pulser affecting the signal from the strain gages, induction pick-up and the thermocouple. This was a real-life instrumentation problem and had to be handled very carefully.

The signals from each of the instruments was observed on an oscilloscope. The effect of increasing voltage and variable frequency and pulse-width was carefully noted. It was found that the signal from the strain gauges had the maximum noise riding on it.

The options available were to either filter the noise using software-filtering, to use a low-pass filter or to rewire the connections using a shielded cable. An averaging subroutine was added to the software used to collect the data wherein a sample of 1000 data points was evaluated a running average of these was used to provide the necessary data value. Software filtering was also used to avoid the spikes corresponding to the high voltage pulses. The noise was also considerably reduced by isolating the strain gages and other instrumentation from the pulser and using shielded cable for all instrumentation. The high voltage wire was replaced by using 52-ohm RG8 RF co-axial cable with PL-259 connectors.

After the corrective measures were affected, the noise was found to be negligible for the voltages and frequencies at which the tests were conducted.

BIBLIOGRAPHY

Block H., Kelly J.P., Quinn A. and Watson T., April 1989, "Materials and Mechanisms in Electrorheology", *Langmuir* 6, No.1, 1990, pp. 6-15.

Brown A.S., March 1990, "Materials get Smarter", *Aerospace America*, pp. 30-35.

Dalal A.F., 1989, "Electrorheological (ER) Fluids and it's Automotive Applications", Project Report, Automobile Engineering (B.E.), University of Bombay, India.

Discover Magazine, September 1988, "Liquid Assets".

Gandhi M.V., Thompson B.S., *Smart Materials and Structures*, New York: Chapman and Hall. Active Sensing and Reactive Smart Structures, pp. 105-118.

Gandhi M.V., Thompson B.S. and Choi S.B., December 1989, "New Generation of Innovative Ultra-Advanced Intelligent Composite Materials Featuring Electro-Rheological Fluids : An Experimental Investigation", *Journal of Composite Materials* 23, pp. 1232-1255.

Gast A.P. and Zukoski C.F., 1989, "Electrorheological Fluids as Colloidal suspensions", *Advances in Colloid and Interface Science*, pp. 153-158, 184-189.

Klass, D.L. and Martinek,T.W.,1967a, "Electroviscous Fluids.I.Rheological Properties", *J.Applied Physics* 38, pp. 67-74.

Klass, D.L. and Martinek,T.W., 1967b, "Electroviscous Fluids.II. Electrical Properties", *J.Applied Physics* 38, pp. 75-80.

Lingard S., Bullough W.A. and Shek W.M.,May 1989, "Tribological Performance of Electrorheological Fluid", *J. Applied Physics* 22, pp. 1639-1645.

Stangroom J. E., "Electrically Variable Linkage Joints", $_{(12)}$UK Patent$_{(19)}$GB$_{(11)}$ 2118741.

Webb N., Electrorheological Fluids, *Chemistry in Britain*, April 1990, pp. 338-340.

Winslow,W.M., 1949 "Induced Fibration of Suspensions", *Journal of Applied Physics* 20, pp. 1137-1140.

Wong W. and Shaw M.T., "The Role of Water in Electrorheological Fluids", pp. 333-337.